THE INFRARED SPECTRUM OF CYANATE ION IN DIFFERENT ENVIRONMENTS

by

ARTHUR GEORGE MAKI, JR.

A THESIS

submitted to

OREGON STATE COLLEGE

in partial fulfillment of
the requirements for the
degree of

DOCTOR OF PHILOSOPHY

June 1960

APPROVED:

Redacted for Privacy

Professor of Chemistry

In Charge of Major

Redacted for Privacy

Chairman of Department of Chemistry

Redacted for Privacy

Chairman of School Graduate Committee

Redacted for Privacy

Dean of Graduate School

Date thesis is presented August 19, 1959

Typed by Lilah N. Potter

TABLE OF CONTENTS

LIST OF TABLES

LIST OF FIGURES

THE INFRARED SPECTRUM OF CYANATE ION IN DIFFERENT ENVIRONMENTS

I. INTRODUCTION

A. Infrared Spectroscopy and Molecular Structure

One of the objectives of science is the ultimate understanding of nature and the world about us and the utilization of this understanding for the good of mankind. Throughout the ages a number of philosophical, experimental, and theoretical (a more rigorous form of philosophy) techniques have been developed to give us a clearer insight into the nature of the world about us.

In recent years a particularly prolific field of scientific endeavor has been that of the elucidation of the structure of matter. The term matter here is meant to denote the substance of the macroscopic world as we know it. The study of the structures of matter can generally be divided into the two broad and perhaps overlapping fields of nuclear physics and chemical physics. The latter term might perhaps be more appropriately called molecular physics. This thesis deals with a phase of the latter catagory.

Among the rapidly growing multitude of techniques for the determination of molecular structure one of the

more versatile techniques is that which utilizes the absorption of infrared radiation to determine the structure of the absorbing material. Most other techniques suffer from severe limitations on the nature of the material being studied. Electron diffraction work, for example, requires that the material be in a gaseous state, x-ray diffraction on the contrary requires solid materials and in addition requires extreme care to differentiate between certain atoms. It is in fact practically hopeless for treating hydrogen containing compounds in a complete manner. On the other hand infrared spectroscopy (if microwave spectroscopy is excepted) is equally good for use with any physical state, with some reservations to be discussed below. Unfortunately infrared absorption gives no direct information on the structure of a particular substance but rather indicates the symmetry of the structure and the nature of the various valence bonds. In addition it is becoming increasingly evident that the study of infrared absorption can give some knowledge of the environment of the molecule or molecular group under study. The study of the absorption spectrum of solids is sometimes complicated due to perturbations arising from the environment whereas the absorption of gases, if at sufficiently low pressures, is essentially that of a molecule free from external

perturbations. As yet the exact nature and result of these environmental effects is very poorly understood. It is the purpose of this thesis to add to the general knowledge regarding the effect of the environment on infrared absorption and at the same time, as always accompanies an increase of knowledge, to indicate the need for a more complete understanding of the cause and effect of intermolecular forces.

In-as-much as the absorption and emission of infrared radiation is caused by changes in the excited vibrational quantum levels of a molecule, the study of infrared spectroscopy is in reality a study of the natural vibrational frequencies of the molecule in question. These vibrational frequencies are of course governed by the kinetic and potential energies of the atoms of the molecule and consequently are related to the forces between atoms within a molecule as well as between molecules. Thus considerable information may be gained from infrared spectroscopy regarding the valence bonds of a compound. So far the reverse process has defied success so that even for the simplest cases it is not possible to predict quantitatively the vibrational behavior of a molecule. To be sure a qualitative estimate of the infrared spectrum of a molecule of known structure can be made on an empirical basis, but this process does not boast of

a true insight into the basic physical principles involved.

In order to understand more clearly the factors important to an *a priori* calculation of the force constants involved in the molecular vibrations, it is helpful to make detailed studies of the vibrations of a number of different simple molecules. As yet very few simple molecules have been studied in detail. This thesis treats the cyanate ion as it is one of a series of molecular entities isoelectronic with carbon dioxide which has been very thoroughly treated in the classic work of Dennison *et al.* (2, p. 716-723; 3, p. 99-104; 17, p. 179-188). Unfortunately the cyanate ion unlike the gaseous CO_2 molecule cannot be studied in isolated form, but must always be in close association with perturbing influences such as other ions in the solid, or with solvent molecules in a liquid solution.

Because the structure of solids is more ordered and in some respects better understood than liquids, the use of solid solutions of cyanate ions dissolved in alkali halides is here used as a means of isolating the cyanate ions from each other and thus eliminating any possibility of perturbations due to dipole-dipole coupling between cyanate ions. In the course of this work this technique has been found to give infrared absorption bands

resolved to a degree hitherto unobtainable with solid samples. Thus it has been found possible to obtain information as to the influence of various environments on the infrared absorption spectrum of the cyanate ion and it is to be hoped that this study may shed some light upon the extent to which the molecules are affected by their environment.

B. Previous Investigations of the Structure of the Cyanate Ion

Various bits of chemical information tell us that the cyanate ion is composed of just three atoms, one carbon atom with an oxygen atom on one side and a nitrogen atom on the other. Thus there is a carbon-nitrogen bond which is in many respects similar to the cyanide bond; and a carbon-oxygen bond somewhat like the bonds in carbon dioxide. By analogy with CO_2 and HCN one would expect the cyanate ion to have a linear configuration. One would also expect that the structure of the ions could be represented by the following three resonance structures:

$$\bar{O}-C\equiv N \qquad (A)$$

$$O=C=\bar{N} \qquad (B)$$

$$\overset{+}{O}\equiv C-\bar{\bar{N}} \qquad (C)$$

other possible resonance structures being deemed unimportant in accordance with Pauling's adjacent charge rule (40, p. 200). Of these structures it might be expected that the first (A) should be the most important due to the greater electronegativity of the oxygen atom. If this were so one would expect the C-N bond distance to be close to that of a C-N triple bond while the C-O bond distance would be expected to be greater than that of a double bond.

Hendricks and Pauling (26, p. 2912-2916) have studied the structure of potassium cyanate by means of x-ray diffraction and found that the cyanate ion is indeed linear. It is unfortunate that x-ray diffraction is unable to detect the difference between the three atoms of the cyanate ion without going to a great deal of work. For this reason Hendricks and Pauling were unable to determine the interatomic distances other than to say that they are both nearly the same and equal to about 1.16 Å. M. Bassière (9, p. 1309-1311) later studied the structure of sodium cyanate and came to the conclusion that the C-N bond distance is 1.21 Å while that for C-O is 1.13 Å. Comparison with Table 1 shows that the work of M. Bassière gives bond lengths which seem to favor the resonance structure B. It might here be added, however, that Bassière has also reported (8, p. 1309-1311)

Table 1

Covalent Bond Distances (40, p. 169)

C—N	-------	1.47 A	C—O	-------	1.43 A
C=N	-------	1.265 A	C=O	-------	1.215 A
C≡N	-------	1.15 A	C≡O	-------	1.10 A

that the azide ion is not symmetrical. This is most certainly an erroneous result and consequently casts doubt upon the accuracy of the cyanate work.

The earliest vibrational studies of the cyanate ion consisted of a very cursory examination of the Raman spectrum of aqueous solutions. The most thorough of these works were those due to J. Goubeau (23, p. 912-919), Pal and Sen Gupta (39, p. 30) and Forrest Cleveland (11, p. 622-623). Table 2 summarizes the results of these workers. Because this early work was carried out in aqueous solution, the hydrolysis of cyanate was a major problem. This hydrolysis according to the equations

$$KNCO + 3H_2O \rightleftharpoons KHCO_3 + NH_4OH$$

$$2KNCO + 4H_2O \rightleftharpoons K_2CO_3 + (NH_4)_2CO_3$$

gives rise to ammonium and carbonate ions which cause a number of spurious absorption bands. In spite of the recognition of this hydrolysis, some of these early workers attributed a band at 850 cm^{-1} to cyanate whereas

Table 2

Assigned Fundamental Vibrational Frequencies

Assignment	F. Cleveland (11, p. 622-623) (Raman)	Pal and Sen Gupta (39, p. 30) (Raman)	J. Goubeau (23, p. 919) (Raman)	D. Williams (52, p. 2442-2444) (I. R.)	This Work (I. R.)
ν_1	----	1229 1314	857	870	1205.5 1292.6
ν_2	----	838	($2\nu_2$ = 970)	----	629.4
ν_3	2171	2183	2192	2180	2169.6

it is most certainly due to carbonate ions. Other workers disregarded the absorption bands at 1225 and 1315 cm^{-1} as being due to other impurities. Part of the confusion which arose was due to the conviction that only three fundamentals should be observed in the region around 500, 1000, and 2100 cm^{-1}. It now appears certain that resonance between a fundamental and an overtone gives rise to a fourth strong band in addition to the expected three. The only previous infrared study of the cyanate ion was that due to D. Williams (52, p. 2442-2444). Williams' work was done in the infancy of infrared spectroscopy and consequently the sensitivity and resolution of his equipment was rather low by present standards. This work was also done in aqueous solution; hence the frequency range of the work was limited by the strong absorption of the water.

L. H. Jones (32, p. 1069-1072; 33, p. 1234-1236) has recently made a thorough study of the thiocyanate ion. The results of this work indicate that the relative importance of resonance structures similar to A, B, and C are respectively 71%, 12%, and 17%. Because of the similarity between the oxygen and sulfur atom, one might expect roughly the same percentages to apply for the cyanate ion.

II. THEORY OF MOLECULAR VIBRATIONS

A. Elementary Theory of Infrared Spectroscopy

In order for infrared radiation to be absorbed in appreciable quantity it is necessary for the radiation to produce a charge in the dipole of the molecule. In the frequency range of infrared radiation this charge of dipole may be accomplished either by increasing the rotational energy of a polar molecule or by promoting the molecule to a higher vibrational level for vibrations which cause a change of the over-all dipole of the molecule. Most of this work is concerned with vibrational spectra, consequently the following discussion will ignore rotational absorption.

A system of N particles has 3N degrees of freedom; however, for a molecule containing N atoms, six degrees of freedom may be allotted to the translation and rotation of the molecule as a whole thus leaving 3N-6 internal degrees of freedom for the molecule (3N-5 for linear molecules). These 3N-6 (or 3N-5) degrees of freedom are called vibrational degrees of freedom as they may be used up by a complete description of the vibrational motions of the atoms.

One may write the equation for the kinetic energy

of a molecule as:

$$2T = \sum_{i=1}^{3N} \dot{q}_i^2$$

where the q_i's are mass weighted coordinates such as

$$q_1 = \sqrt{m_1}\ \Delta x_1 , \quad q_2 = \sqrt{m_1}\ \Delta y_1 , \quad \text{etc.}$$

The potential energy may be written as a power series of the displacement coordinates as

$$2V = 2V_0 + 2\sum_{i=1}^{3N} \left(\frac{\partial V}{\partial q_i}\right)_0 q_i + \sum_{i,j=1}^{3N} \left(\frac{\partial^2 V}{\partial q_i\, \partial q_j}\right)_0 q_i q_j + \text{higher terms}$$

the subscript o denoting the equilibrium position.

If we choose the equilibrium position as the zero of potential energy then $V_0 = 0$. Furthermore the equilibrium position means that the energy is at a minimum so that $\left(\frac{\partial V}{\partial q_i}\right)_0 = 0$. Therefore if cubic and higher terms are neglected

$$2V = \sum_{i,j=1}^{3N} f_{ij}\, q_i\, q_j$$

where

$$f_{ij} = f_{ji} = \left(\frac{\partial^2 V}{\partial q_i\, \partial q_j}\right)_0$$

If we now apply Lagranges equations

$$\frac{d}{dt}\frac{\partial T}{\partial \dot{q}_i} + \frac{\partial V}{\partial q_i} = 0 \qquad i = 1, 2, \cdots, 3N$$

we will obtain

$$\ddot{q}_i + \sum_{j=1}^{3N} f_{ij} q_j = 0 \qquad i = 1, 2, \cdots, 3N$$

This set of differential equations has the solutions

$$q_i = A_i \cos(\lambda^{\frac{1}{2}} t + \epsilon) \qquad i = 1, 2, \cdots, 3N$$

for which substitution in the differential equations yields

$$\sum_{i=1}^{3N} (f_{ij} - \delta_{ij}\lambda) A_i = 0 \qquad j = 1, 2, \cdots, 3N$$

The λ's may be obtained by solving the secular equation

$$\begin{vmatrix} f_{11}-\lambda & f_{12} & f_{13} & \cdots & f_{13N} \\ f_{21} & f_{22}-\lambda & f_{23} & \cdots & f_{23N} \\ \vdots & \vdots & \vdots & \vdots & \vdots \\ f_{3N1} & f_{3N2} & f_{3N3} & \cdots & f_{3N3N}-\lambda \end{vmatrix} = 0$$

and, using these values of λ, the amplitudes A_i may be found except for a normalization factor.

Due to the fact that we are here dealing with molecules for which the coordinates of the atoms are not independent it will be found that the above secular equation

yields only 3N-6 (3N-5 for linear molecules) non-zero λ's.

The zero roots of the secular equation may be eliminated by making a different choice of coordinates such that 3N-6 (or 3N-5) independent coordinates are used. One such set of coordinates called the normal coordinates may be chosen such that the form of the potential and kinetic energy equations is the same as that given above. Thus the normal coordinates obey the equations

$$Q_k = A_k \cos(\lambda_k^{\frac{1}{2}} t + \epsilon) \qquad k = 1, 2, \cdots, 3N-6$$

or since

$$Q_k = \sum_{i=1}^{3N} l_{ik} q_i$$

then

$$\sum_{i=1}^{3N} l_{ik} q_i = A_k \cos(\lambda_k^{\frac{1}{2}} t + \epsilon)$$

so that for a given solution λ_k the different q_i are changing with the same frequency and phase thus executing simple harmonic motion. It may happen that two or more λ_k's are equal thus giving rise to two or more normal coordinates with the same frequency. These are then called degenerate vibrations as they are found to represent states of equal energy.

If wave mechanics are applied using normal

coordinates and the kinetic and potential energies,

$$2T = \sum_{k=1}^{3N-6} \dot{Q}_k^2$$

and

$$2V = \sum_{k=1}^{3N-6} \lambda_k Q_k^2 ,$$

the vibrational wave equation for the molecule will then be

$$-\frac{h^2}{8\pi^2} \sum_{k=1}^{3N-6} \frac{\partial^2 \psi_v}{\partial Q_k^2} + \frac{1}{2} \sum_{k=1}^{3N-6} \lambda_k Q_k^2 \psi_v = W_v \psi_v$$

where it is assumed that the wave function ψ is separable as

$$\psi = \psi_v \psi_R \cdots$$

and W_v represents the energy of the corresponding state.

If it is also assumed that these are further separable so that

$$\psi_v = \psi(Q_1)\psi(Q_2) \cdots \psi(Q_{3N-6})$$

and

$$W_v = W(Q_1) W(Q_2) \cdots W(Q_{3N-6})$$

then the wave equation is separable into the equations

$$-\frac{h^2}{8\pi^2} \frac{d^2\psi(Q_k)}{dQ_k^2} + \frac{1}{2}\lambda_k Q_k^2 \psi(Q_k) = W(Q_k)\psi(Q_k)$$

This is the differential equation for a harmonic oscillator for which the energy levels are found to be

$$W_i = (v + \tfrac{1}{2}) h \nu_i \qquad \begin{matrix} v = 0, 1, 2, \cdots \\ i = 1, 2, \cdots, 3N-6 \end{matrix}$$

where the ν_i's are the classical vibrational frequencies of the system and h is Plank's constant.

By determining the vibrational frequencies ν_k it is possible to calculate the force constants λ_k for the normal coordinates Q_k. However, inasmuch as the form of $Q_k = \sum_{i=1}^{3N} l_{ik} q_i$ bears no obvious relation to the chemistry of a compound, these force constants are of little value. A more useful force constant would be one which is related to a specific bond or bond angle. For this reason it is more profitable to define a new set of coordinates called internal coordinates. These internal coordinates will then represent changes in bond lengths and angles so that their force constants will denote the ease with which the bonds undergo change, and consequently provide a measure of the difference between bonds.

Rather elegant matrix and group theoretical techniques have been devised to simplify writing out and solving the harmonic oscillator problem in the case of simpler molecules (see Wilson, Decius and Cross (53, p. 1-388)), but as the molecule increases in size and decreases

in symmetry the problem rapidly becomes too complex to solve even with the use of these simplifying techniques. In the relatively simple case of a three atom, linear molecule such as the cynate ion, however, it is not only possible to solve the harmonic oscillator problem, but also to include terms for the anharmonicity. This will be taken up later.

B. Intensity of Infrared Absorption

For radiation with a wave length large with respect to the dimensions of the molecule it can be shown using perturbation theory that the einstein coefficient of absorption is given by the equation

$$B_{m\to n} = \frac{8\pi^3}{3h^2}\left[|(\mu)_{mn}|^2\right]$$

where

$$(\mu)_{mn} = \int \psi_m^* \mu \psi_n \, d\tau$$

or since μ , the electric moment, may be broken up into component vectors,

$$(\mu_x)_{mn} = \int \psi_m^* \mu_x \psi_n \, d\tau \ .$$

This means that if $(\mu)_{mn}$ is zero for a given transition $m \to n$ then no radiation will be absorbed due to that

transition.

It is possible by studying the symmetry of a molecule to determine whether or not the above integral vanishes, thus arriving at a set of selection rules which specify what transitions are capable of absorbing radiation.

A more general selection rule can also be derived irrespective of the molecule involved. The electric moment is defined as $\mu_x = \sum_\alpha e_\alpha x_\alpha$, where we may take the sum over all atoms in a molecule. The effective charge on each atom, e_α , may change as the molecule vibrates in-as-much as the electron distribution may change with change in position of the atoms. This change in effective charge may not be linear and so the electric moment may be best represented by a power series expansion in terms of normal coordinates

$$\mu_x = \mu_x^0 + \sum_{k=1}^{3N-6} \mu_x^{(k)} Q_k + \sum_{i,j=1}^{3N-6} \mu_x^{(i,j)} Q_j Q_i + \cdots$$

where

$$\mu_x^{(k)} = \frac{\partial \mu_x}{\partial Q_k} \qquad \text{and} \qquad \mu_x^{(i,j)} = \frac{\partial^2 \mu_x}{\partial Q_i \, \partial Q_j} = \mu_x^{(j,i)}$$

And similarly for μ_y and μ_z.

If the vibrational portion of the wave function is assumed to be a product of harmonic oscillator functions, then the dipole integral is given by

$$\int \psi_{v'}^{*} \mu_x \psi_v \, d\tau = \mu_x^{0} \int \psi_{v'}^{*} \psi_v \, d\tau + \sum_{k=1}^{3N-6} \mu_x^{(k)} \int \psi_{v'}^{*} Q_k \psi_v \, d\tau$$

$$+ \sum_{i,j=1}^{3N-6} \mu_x^{(i,j)} \int \psi_{v'}^{*} Q_i Q_j \psi_v \, d\tau + \cdots .$$

The first term on the right hand side of this equation is zero unless $V = V'$ due to the orthogonality of the vibrational wave functions; thus this contributes nothing to the absorption. The integral in the second term is non-zero only if $V = V' \pm 1$. This gives rise to absorption due to vibrational quantum number changes of one unit. These are called fundamental absorptions. The third term is zero unless $V = V'$ or $V' \pm 2$ thus giving an absorption for vibrational quantum number jumps of two. Higher terms would of course give rise to absorption due to greater quantum number jumps. In addition the third term will give rise to what are known as combination frequencies due to such integrals as $\int \psi_{v'}^{*} Q_i Q_j \psi_v \, d\tau \quad i \neq j$ for which $V_i = V_i' \pm 1$ and $V_j = V_j' \pm 1$. It will be noted however that the intensity of absorption is also governed by the coefficients of these integrals so that the intensities of the fundamental bands depend on $\mu_x^{(k)}$, $\mu_y^{(k)}$, $\mu_z^{(k)}$ and similarly for the higher terms. Thus selection

rules for the individual molecules may be derived according as $\mu^{(i)}$, $\mu^{(i,j)}$, etc. are zero or non-zero. Since the higher derivatives of the electric moment rapidly diminish in magnitude, the intensities of overtone and combination bands are generally quite small with respect to the fundamental intensities, and the intensities of higher overtones fall off quite rapidly.

In addition to considering the anharmonicity or non-linearity of the electric moment, one could, with considerably more difficulty, consider anharmonicity as it affects the wave function. Anharmonic wave functions would show that the intensity of overtones is also governed somewhat by the dipole derivative $\mu_x^{(i)}$, $\mu_y^{(i)}$, $\mu_z^{(i)}$.

Returning to the expression for the Einstein absorption coefficient, it can be shown that the absorption coefficient (K), or better yet the integrated absorption coefficient is given by

$$\int_{\text{line } v \to v'} K(\nu)\, d\nu = \frac{h\nu_{vv'}}{c} B_{vv'}(N_v - N_{v'})$$

$$= \frac{8\pi^3}{3ch}\, \nu_{vv'}(N_v - N_{v'}) \left|(\mu)_{vv'}\right|^2$$

where $N_{v'}$ equals the number of molecules per unit volume in the state v'. Assuming N_v is much greater than $N_{v'}$

and evaluating the dipole moment matrix element for the transition $v_k \rightarrow v_k + 1$ neglecting terms higher than the second in the electric moment power series gives

$$(\mu)_{v_k+1, v_k} = \mu^{(k)} \left[\frac{h}{8\pi^2 \nu_k} (v_k + 1) \right]^{\frac{1}{2}}$$

therefore

$$\int_{\text{line } v_k \rightarrow v_k+1} K(\nu)\, d\nu = \frac{d N \pi}{3c} \left[(\mu^{(k)})^2 \right] (v_k + 1)$$

where d is the degenerary of the band in question.

Thus we see that the intensity of absorption is proportional to

$$I_k = \left| (\mu^{(k)})^2 \right| = \left(\frac{\partial \mu_x}{\partial Q_k} \right)^2 + \left(\frac{\partial \mu_y}{\partial Q_k} \right)^2 + \left(\frac{\partial \mu_z}{\partial Q_k} \right)^2 .$$

Now since the normal coordinates Q_k are related to internal symmetry coordinates $S_{k'}$, by the transformation equation

$$S_{k'} = \sum_k L_{k'k} Q_k \quad ,$$

we can write

$$I_k = \left(\frac{\partial \mu}{\partial Q_k} \right) \cdot \left(\frac{\partial \mu}{\partial Q_k} \right) = \sum_{k'k''} \left(\frac{\partial \mu}{\partial S_{k'}} \right) \left(\frac{\partial \mu}{\partial S_{k''}} \right) L_{k'k} L_{k''k} .$$

The transformation coefficients $L_{k'k}$ can be shown (53, p. 191-192) to be related to the kinetic energy matrix G and the potential energy matrix F in the following manner

$$\sum_{k} L_{k'k} L_{k''k} = G_{k'k''}$$

and

$$\sum_{k'k''} L_{k'k} F_{k'k''} L_{k''k} = \lambda_k$$

or

$$\sum_{k} L_{k'k} \lambda_k^{-1} L_{k''k} = F_{k'k''}^{-1}$$

Here the λ's are the eigenvalues of the energy equation and are proportional to the square of the frequency of the fundamental vibrations. F is isotopically invariant as it is the force constant matrix, whereas G is not invariant. Summing over all vibrations of a given symmetry species then gives

$$\sum_{k} I_k = \sum_{k'k''} \frac{\partial \mu}{\partial S_{k'}} \frac{\partial \mu}{\partial S_{k''}} \sum_{k} L_{k'k} L_{k''k} = \sum_{k'k''} \frac{\partial \mu}{\partial S_{k'}} \frac{\partial \mu}{\partial S_{k''}} G_{k'k''}$$

and multiplying by λ_k^{-1}

$$\sum_{k} \frac{I_k}{\lambda_k} = \sum_{k'k''} \frac{\partial \mu}{\partial S_{k'}} \cdot \frac{\partial \mu}{\partial S_{k''}} \sum_{k} L_{k'k} \lambda_k^{-1} L_{k''k}$$

$$= \sum_{k'k''} \frac{\partial \mu}{\partial S_{k'}} \frac{\partial \mu}{\partial S_{k''}} F^{-1}_{k'k''} \quad .$$

Subject to the conditions (a) that the molecule should have no dipole moment and/or (b) that the symmetry species over which the summation is carried out should contain no rotation of the molecule, $\frac{\partial \mu}{\partial S_{k'}}$ is independent of isotopic constitution. It thus follows that

$$\sum_{k} \frac{I_k}{\lambda_k}$$

is constant regardless of isotopic content whereas $\sum_{k} I_k$ changes slightly with isotopic substitution because of the variation in the G matrix elements with change in atomic masses.

It should be emphasized, however, that the foregoing intensity rules have been derived assuming the molecule is a harmonic oscillator with no higher order terms in the equation for the electric dipole moment. This means that the rules will not be applicable to combination or overtone absorptions which by their very nature are due to anharmonic vibrations. Nor will the rules hold rigorously for fundamentals in-as-much as the

fundamentals will also have a certain degree of anharmonicity. The rules are, however, probably good to an accuracy of at least 5% in almost all cases.

C. Frequency Product Rule for Isotopic Substitution

The kinetic and potential energies may be expressed in terms of external symmetry coordinates S_k and their conjugate moments P_k by the following equations

$$2V = \sum_{kl} F_{kl} S_k S_l$$

$$2T = \sum_{k} G_{kk} P_k^2$$

Here the F_{kl} are the maxtric elements of the F matrix and G_{kl} are the matrix elements of the G matrix. In the system of external symmetry coordinates the G matrix is in diagonal form with each diagonal term being the reciprocal mass μ_k of one atom of a single equivalent set of atoms. The product of the eigenvalues is then equal to the determinant of the coefficients of the secular equation. Thus

$$|FG| = |F| \cdot \mu_1 \mu_2 \cdots \mu_k = \lambda_1 \lambda_2 \cdots \lambda_k$$

where

$$\lambda_k = 4\pi^2 \nu_k^2 = 4\pi^2 c^2 \omega_k^2$$

Since the force constant matrix F is isotopically invariant due to the use of symmetry coordinates then

$$\frac{\mu_1 \mu_2 \cdots \mu_n}{\mu_1' \mu_2' \cdots \mu_n'} = \frac{\lambda_1 \lambda_2 \cdots \lambda_n}{\lambda_1' \lambda_2' \cdots \lambda_n'}$$

where the prime indicates the value for an isotopically substituted molecule. Since external symmetry coordinates still retain terms for translational and rotational motion for which the characteristic values are zero, it is necessary to remove these zero roots by some gambit.

By introducing weak forces which convert these translational and rotational motions into low frequency vibrations and then taking the limit of these vanishing forces the ratio of the translational frequencies are

$$\frac{\lambda_t'}{\lambda_t} = \frac{M}{M'}$$

and for rotational frequencies

$$\frac{\lambda_R}{\lambda_R'} = \frac{I'}{I} .$$

Here M is the total mass of the molecule and I is the moment of inertia with respect to the proper principal axis.

Thus if all the rotational and translational modes are removed the Redlich-Teller product rule is obtained

$$\prod_{k=1}^{3N-6} \frac{\omega_k}{\omega'_k} = \prod_{k=1}^{3N-6} \left(\frac{\lambda_k}{\lambda'_k}\right)^{\frac{1}{2}} = \prod_{i=1}^{3N} \left(\frac{m'_i}{m_i}\right)^{\frac{1}{2}} \left(\frac{M}{M'}\right)^{3/2} \left(\frac{I_x I_y I_z}{I'_x I'_y I'_z}\right)^{3/2}$$

Since the secular equation is factored according to symmetry sub-groups, the above product may also apply only to a given symmetry group provided care is taken to consider possible symmetry changes due to isotopic substitution.

This product rule should hold quite rigorously for the frequencies of infinitesimal displacement, but will be only approximate for the frequencies of the fundamental absorption peaks due to the anharmonicity of any finite vibrational motion.

D. Potential Function Including Anharmonicity

Normally in more complex molecules the problem of determining the force constants is greatly simplified by considering the molecule to be a harmonic oscillator. Thus the potential energy function for vibration only contains quadratic terms. For simpler molecules it is sometimes possible to obtain enough data to allow the evaluation of cubic and quartic terms in the potential function. One of the first molecules to be so treated

was carbon dioxide. In this case the symmetry of the molecule limits the number of possible potential terms to twelve (three quadratic, three cubic, and six quartic). By the observation of a sufficient number of overtones, and inclusion of certain vibration-rotation interaction relations, Adel and Dennison (2, p. 716-723; 3, p. 99-104) were able to evaluate all twelve of these potential terms.

The case of the cyanate ion is not so fortunate in that it is of lower symmetry and consequently the potential energy expression will contain more cross terms. In the case of CO_2 the symmetry gives rise to an additional simplification in that a set of normal coordinates is easily constructed from the changes of a set of internuclear distances. In the cyanate ion on the other hand the normal coordinates for vibration are complicated combinations of changes in the internuclear distances. Because of the symmetry of the carbon dioxide molecule, Adel and Dennison were able to define a set of coordinates which would give no cross terms in the quadratic portion of the potential function. Their potential function had the form:

$$\frac{2V}{h} = \omega_1\sigma^2 + \omega_2\rho^2 + \omega_3\xi^2 + a\sigma^3 + b\sigma\rho^2 + c\sigma\xi^2 + d\sigma^4 + e\rho^4 + f\xi^4 + g\sigma^2\rho^2 + i\xi^2\sigma^2 + j\rho^2\xi^2 \qquad (1)$$

where they used dimensionless coordinates such that σ is proportional to the relative separations of the end atoms, ξ is proportional to the relative displacement of the interior atom with respect to the center of mass of the end atoms measured parallel to the axis of the molecule, and ρ and ϕ are proportional to the polar coordinates of the carbon atom in a plane perpendicular to the axis of the molecule, the origin lying at the center of mass of the end atoms. It may be noted that the potential energy is independent of the angle ϕ and of odd powers of ρ and ξ .

Referring to Figure 1 one can see that the normal modes ω_1 and ω_3 in cyanate ion represent simultaneous changes in both ξ and σ . Consequently, if the potential energy function for cyanate ion is written in normal coordinate form

$$\frac{2V}{h} = \omega_1 Q_1^2 + \omega_2 (Q_{2a}^2 + Q_{2b}^2) + \omega_3 Q_3^2 + \sum_{ijk} q_{ijk} Q_i Q_j Q_k + \sum_{ijkl} h_{ijkl} Q_i Q_j Q_k Q_l + \cdots \qquad (2)$$

where the Q's are the normal coordinates, then the constants for the Q_1 and Q_3 coordinates are really combinations of the constants for σ and ξ in the potential function due to Dennison and Adel. Furthermore, since

Figure 1

Normal Vibrational Modes for
Carbon Dioxide and Cyanate Ion

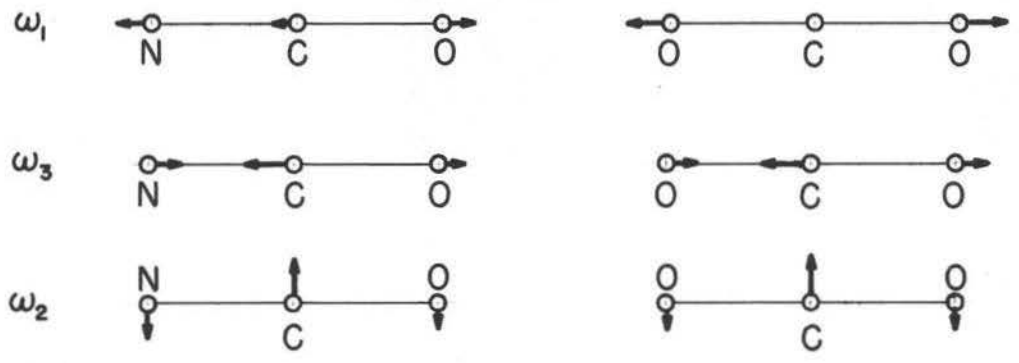

the form of the normal coordinates will change upon isotopic substitution in the cyanate ion, the equations relating Q_1 and Q_3 to σ and ξ will change and consequently so will the equations relating the potential constants for the two sets of coordinates. For this reason it is evident that while the potential constants of Adel and Dennison should not change for an isotopic substitution which retains the symmetry of the molecule, an isotopic substitution in the cyanate ion would be expected to change the constants in the potential energy equation containing the normal coordinates. However, it should be possible to change from these constants to a different set based upon the bond deformations of the molecule or ion. This latter set of potential constants

based upon so called internal coordinates should be invariant with respect to isotopic substitution.

In-as-much as the number of potential constants for most molecules is so large there is not usually enough information to allow an evaluation of them. One can, however, make a judicious choice of the constants most likely to be of appreciable size and assume all the others to be zero. It can in addition be shown that the vibrational frequencies of a molecule or ion can be more easily represented by an energy equation of the form

$$E = h\nu_1(v_1 + \tfrac{d_1}{2}) + h\nu_2(v_2 + \tfrac{d_2}{2}) + h\nu_3(v_3 + \tfrac{d_3}{2})$$

$$+ \sum_i \sum_j x_{ij}(v_i + \tfrac{d_i}{2})(v_j + \tfrac{d_j}{2}) + \sum_{i,j} g_{ij}\, l_i\, l_j$$

where d_i is the degeneracy of the i'th mode and the x_{ij}'s can be related to the potential constants. The smaller number of x_{ij}'s makes this a very convenient way of comparing molecules. The relationship between the x_{ij}'s and the potential constants may be derived in the following way.

Since the solution of the Schroedinger equation using a potential function for an anharmonic oscillator is extremely difficult, the use of perturbation theory is usually made. Thus if the potential energy equation

is assumed to be of the form indicated by equation 2 and the initial (quadratic) terms are large with respect to the later summations, we may first compute the energy due to the hamiltonian containing only the first terms and add onto this the energy terms due to perturbations arising from the cubic and quartic potential terms.

The Schroedinger equation including just the quadratic terms is easily recognized as the differential equation for a harmonic oscillator giving rise to the energy equation:

$$W = h\nu_1(v_1 + \tfrac{1}{2}) + h\nu_2(v_2 + 1) + h\nu_3(v_3 + \tfrac{1}{2}).$$

Since Q_2 is a degenerate mode, it gives rise to the term $v_2 + 1$ rather than a term similar to that of Q_1 and Q_3 which have a $+\frac{1}{2}$ rather than a +1.

Inclusion of the cubic and quartic terms in a first order perturbation treatment gives rise to additional equations of the type:

$$E'_v = \int \psi_v^* H' \psi_v \, d\tau$$

or, if corresponding perturbation terms in the kinetic energy equation are neglected

$$E'_v = \sum_{ijk}^{3} q_{ijk} \int \psi_v^* Q_i Q_j Q_k \psi_v \, d\tau$$

$$+ \sum_{ijkl} h_{ijkl} \int \psi_v^* Q_i Q_j Q_k Q_l \psi_v \, d\tau .$$

Since the ψ_v is considered separable into ψ's for each normal mode

$$\psi_v = \psi_{v_1} \cdot \psi_{v_2} \cdot \psi_{v_3}$$

then the perturbation energy terms consist of a few different types of integrals, namely:

$$\int \psi_v^* Q_i Q_j^2 \psi_v \, d\tau = 0 \qquad i \neq j$$

$$\int \psi_v^* Q_i^3 \psi_v \, d\tau = 0$$

$$\int \psi_v^* Q_i Q_j Q_k \psi_v \, d\tau = 0 \qquad i \neq j \neq k$$

$$\int \psi_v^* Q_i Q_j Q_k^2 \psi_v \, d\tau = 0 \qquad i \neq j \neq k$$

$$\int \psi_v^* Q_i Q_j^3 \psi_v \, d\tau = 0 \qquad i \neq j$$

$$\int \psi_v^* Q_i^4 \psi_v \, d\tau = \left[(v_i + \tfrac{1}{2})^2 + \tfrac{1}{4} \right] \frac{3h^2}{32\pi^4 \nu_i^2} \qquad i = 1 \text{ or } 3$$

$$\int \psi_v^* Q_i^2 Q_j^2 \psi_v \, d\tau = (v_i + \tfrac{1}{2})(v_j + \tfrac{1}{2}) \frac{h^2}{16\pi^4 \nu_i \nu_j} \qquad \begin{matrix} i = 1 \\ j = 3 \end{matrix}$$

$$\int \psi_v^* Q_i^4 \psi_v \, d\tau = (3v_i^2 + 6v_i + 4 - e^2) \frac{h^2}{32\pi^4 \nu_i^2} \qquad i = 2$$

$$\int \psi_v^* Q_i^2 Q_j^2 \psi_v \, d\tau = (v_i + \tfrac{1}{2})(v_j + 1) \frac{h^2}{16\pi^4 \nu_i \nu_j}$$

$i = 1$ or 3
$j = 2$

These integrals were evaluated for the case of triatomic linear molecules for which the wave functions for the Q_1 and Q_3 coordinates are Hermite polynomials while the wave functions for the degenerate coordinate Q_2 are Laguerre polynomials also known as two dimensional Hermite polynomials. These integrals were evaluated according to tables found in Wilson, Decius, and Cross (53, p. 290-291) and T. Wu (55, p. 55).

It is apparent that the energy correction due to this first order perturbation treatment only contains a few of the potential terms because all the integrals involving cubic terms vanish as do many of the quartic integrals.

To arrive at an energy equation involving cubic terms it is necessary to resort to a second order perturbation treatment. This gives rise to perturbation energies of the form

$$E_v' = \sum_{v'}{}' \frac{\int \psi_{v'}^* H' \psi_v \, d\tau \int \psi_v^* H' \psi_{v'} \, d\tau}{E_{v'}^\circ - E_v^\circ}$$

where the prime on the summation sign denotes exclusion of $v' = v$.

As with the first order perturbation this gives three general types of integrals:

$$\int \psi_{v'}^{*} Q_1 Q_2 Q_3 \psi_v \, d\tau = 0$$

$$\int \psi_{v'}^{*} Q_i Q_j^2 \psi_v \, d\tau = 0 \qquad \text{for} \begin{cases} v_i' \neq v_i \pm 1, & i = 2 \\ v_j' \neq v_j \text{ or } v_j \pm 2 \end{cases}$$

$$\int \psi_{v'}^{*} Q_i^3 \psi_v \, d\tau = 0 \qquad \text{for} \begin{cases} v_i' \neq v_i \pm 1, \text{ or } v_i \pm 3 \\ i = 2 \end{cases}$$

The evaluation of all these second order energy terms shown that, if non-zero, they contain only quadratic functions of $(v_i + 1)$ or $(v_i + \frac{1}{2})$. Consequently the energy equation can be represented to a high degree of approximation by an equation of the type

$$\frac{E}{hc} = \sum_{k=1}^{3N-6} \omega_k \left(v_k + \frac{g_k}{2}\right) + \sum_{k=1}^{\ell} \sum_{\ell=1}^{3N-6} \chi_{k\ell} \left(v_k + \frac{g_k}{2}\right)\left(v_\ell + \frac{g_\ell}{2}\right).$$

For linear molecules the summation is carried through 3N-5 terms. The g_k is the degeneracy of the k'th vibration.

For molecules possessing some elements of symmetry

the number of potential constants can usually be reduced. In the cyanate ion for instance the bending vibration of the molecule gives rise to a potential energy which must be independent of the direction of vibration (up or down) so that Q_2 must always appear as an even power. Thus for the cyanate ion the complete potential energy term through the quartic terms is

$$2V = \omega_1 Q_1^2 + \omega_2 (Q_{2a}^2 + Q_{2b}^2) + \omega_3 Q_3^2 + g_{111} Q_1^3 + g_{333} Q_3^3$$
$$+ g_{122} Q_1 (Q_{2a}^2 + Q_{2b}^2) + g_{133} Q_1 Q_3^2 + g_{322} Q_3 (Q_{2a}^2 + Q_{2b}^2)$$
$$+ g_{311} Q_3 Q_1^2 + h_{1111} Q_1^4 + h_{2222} (Q_{2a}^4 + 2 Q_{2a}^2 Q_{2b}^2 + Q_{2b}^4) + h_{3333} Q_3^4$$
$$+ h_{1322} Q_1 Q_3 (Q_{2a}^2 + Q_{2b}^2) + h_{2233} Q_3^2 (Q_{2a}^2 + Q_{2b}^2) + h_{1133} Q_1^2 Q_3^2$$
$$+ h_{1122} Q_1^2 (Q_{2a}^2 + Q_{2b}^2) + h_{1333} Q_1 Q_3^3 + h_{3111} Q_3 Q_1^3 .$$

To evaluate these 18 constants would be quite difficult for a molecule containing only three different fundamental vibrational frequencies so that I have chosen to evaluate the anharmonicity constants in the energy expression arrived at above. A table of these constants is included along with other pertinent information in the section on experimental results.

E. Fermi Resonance

It will be noted that in the second order perturbation energy term given above the denominator is the difference between the unperturbed energies of the two levels considered. If this energy difference becomes small, then the perturbation term itself becomes large and the validity of the method breaks down. This then becomes a problem involving accidentally degenerate (or nearly degenerate) energy levels. This type of resonance was first proposed by Fermi (20, p. 250-259) as the explanation for two strong raman bands at 1388 and 1285 cm^{-1} in carbon dioxide where only one Raman line due to the symmetric stretching fundamental is expected. The explanation proposed by Fermi was that this doublet is due to the mutual perturbation or resonance between the first overtone of the banding mode (expected at about 1330 cm^{-1}) and the symmetric stretch fundamental. The resonance causes both vibrational modes to contribute to each band so that the intensities are nearly equal whereas the overtones would normally be expected to be very weak.

This resonance was treated more thoroughly by Dennison and Adel (2, p. 716-723; 17, p. 179-188) with the result that the experimentally observed spectrum could be rather accurately predicted. Following the general

spirit of the treatment of Dennison the Fermi interaction expected for the cyanate ion will now be derived.

If one considers only the cubic terms, the only second order perturbation term which becomes large for the resonant frequencies $2\nu_2$ and ν_1 is $g_{122} Q_1 Q_2^2$.

Thus the perturbed energies W_1, W_2 can be found from the unperturbed energies W_1°, W_2° and the integrals $W_{12} = g_{122} \int \psi^*_{\substack{\nu_1, \ell \\ \nu_2 \\ \nu_3}} Q_1 Q_2^2 \psi_{\substack{\nu_1, -1 \\ \nu_2 \ell+2 \\ \nu_3}} d\tau$ by the secular determinant

$$\begin{vmatrix} W_1^\circ - W & W_{12} \\ W_{12} & W_2^\circ - W \end{vmatrix} = 0 .$$

Upon evaluating this integral one finds

$$W_{12} = - \frac{h^{3/2}}{16\sqrt{2}\,\pi^3 \nu_1^{1/2} \nu_2} \nu_1^{1/2} \left[(\nu_2 + 2)^2 - \ell^2 \right]^{1/2} g_{122} .$$

The Fermi resonant triplet due to the overtones $2\nu_1$, $\nu_1 + 2\nu_2^\circ$, $4\nu_2^\circ$ may be calculated by a simple extension of the above determinant to get

$$\begin{vmatrix} W_1^\circ - W & W_{12} & W_{13} \\ W_{12} & W_2^\circ - W & W_{23} \\ W_{13} & W_{23} & W_3^\circ - W \end{vmatrix} = 0 .$$

where the terms W_{12} and W_{23} are the same as W_{12} above except that v_1 and v_2 will be different. The integral

$$W_{13} = g_{122} \int \psi^{*}_{\substack{v_1 \\ v_2 \\ v_3}} Q_1 Q_2^2 \psi_{\substack{v_1-2 \\ v_2+4 \\ v_3}} d\tau$$

vanishes.

Because the use of the single cubic term g_{122} gives calculated resonance interactions consistently too large for all but the lowest combination bands, it has seemed advisable to include a quartic or higher term in the calculation of the Fermi interaction. Upon examination of the quartic terms it is found that none will give a contribution to the energy so that it is necessary to go on to the quintic terms to find the next non-zero contribution. Among the quintic terms the largest contribution will probably be due to the term g_{12222} as the interaction integral involving this term will have a large coefficient for large v_2 . Combining this with the above mentioned cubic term the two dimensional secular determinant will contain the element

$$W_{12} = g_{122}\int \psi^{*}_{\substack{v_1 \\ v_2^{\ell} \\ v_3}} Q_1 Q_2^2 \psi_{\substack{v_1-1 \\ v_2^{\ell+2} \\ v_3}} d\tau + g_{12222}\int \psi^{*}_{\substack{v_1 \\ v_2^{\ell} \\ v_3}} Q_1 Q_2^4 \psi_{\substack{v_1-1 \\ v_2^{\ell+2} \\ v_3}} d\tau$$

$$= -g_{122}\frac{h^{3/2}}{16\sqrt{2}\,\pi^3 \nu_1^{1/2}\nu_2}\, v_1^{\frac{1}{2}}\left[(v_2+2)^2-\ell^2\right]^{\frac{1}{2}}$$

$$-g_{12222}\frac{h^{5/2}}{32\sqrt{2}\,\pi^5 \nu_1^{1/2}\nu_2^2}\, v_1^{\frac{1}{2}}(v_2+2)\left[(v_2+2)^2-\ell^2\right]^{\frac{1}{2}}.$$

Likewise the 3 x 3 secular determinant for the resonant triplet has the same additional terms for the W_{12} and W_{23} off-diagonal elements and the off-diagonal element W_{13} still vanishes.

Other quintic terms which would also enter into the Fermi resonance are g_{12233} and g_{11122} for which the coefficients are respectively

$$-\frac{h^{5/2}}{64\sqrt{2}\,\pi^5 \nu_1^{1/2}\nu_2\nu_3}\,(v_3+\tfrac{1}{2})(v_1)^{\frac{1}{2}}\left[(v_2+2)^2-\ell^2\right]^{\frac{1}{2}}$$

and

$$-\frac{3h^{5/2}}{128\sqrt{2}\,\pi^5 \nu_2 \nu_1^{3/2}}\, v_1^{3/2}\left[(v_2+2)^2-\ell^2\right]^{\frac{1}{2}}.$$

The accuracy of the experimental work, however, does not warrant using more than one term beyond the cubic term in the Fermi resonance calculation.

Furthermore, the real justification for using resonance interaction terms beyond the cubic is not that this gives better agreement between experimental and calculated absorptions, but rather that this gives a value for the cubic interaction term which is probably more accurate than would otherwise be obtained. The accuracy of the quintic term itself is however subject to much doubt as there are undoubtedly other perturbing influences of a completely different nature due to the forces exerted by neighboring alkali halide ions in the crystal. Because of the relatively short interionic distances it is expected that anharmonicities due to the neighboring ions restricting the vibrations of the cyanate ion should be of a magnitude comparable to that calculated for the quintic term.

In addition it will be noted that in calculating the perturbation integrals harmonic oscillator wave functions were used. In-as-much as cubic and higher terms were used in the potential energy function, it is obvious that anharmonic oscillator wave functions would be required to give exact results. Consequently it is to be expected that the Fermi resonance terms should not provide complete agreement between experimental and theoretical vibrational frequencies. On the contrary,

it is strange that the agreement is as good as it is. In the more thoroughly studied case of CO_2 the calculated and observed frequencies often deviate by 3, 4 or more cm^{-1}.

On the other hand, in some extremely accurate work done recently on HCN (5, p. 302-307) and C_2D_2 (4, p. 279-283) it has been found that inclusion of such higher order terms results in complete agreement between predicted and observed frequencies for resonant lines.

F. Spectra of Solids

1. Selection Rules

In the gaseous state the molecules are relatively free of external forces and consequently each molecule is free to execute rotational and translational motion thus using up six degrees of freedom (or five in the case of linear molecules). As the gas becomes more dense finally liquifying and then crystallizing due to either increased pressure, decreased temperature, or both, these degrees of freedom become fixed into librational and vibrational motions due to intermolecular forces which tend to limit the motion of the molecules.

The vibrational frequencies due to lattice modes are generally of fairly low frequency being around 25 to

200 cm^{-1}. Similarly the librational frequencies are expected to be quite low although certainly higher than the corresponding rotational frequencies of the free molecule.

A number of theoretical papers have been published on the interaction of vibrations in the solid state. Particularly noteworthy are the papers by Halford (25, p. 8-15; 54, p. 607-616), Hornig (31, p. 1063-1076), and Walnut (50, p. 58-62). Halford and Hornig have been primarily interested in the selection rules applicable to crystals and how these differ from the case of isolated molecules. They have shown that otherwise degenerate vibrational modes may be split due to the site symmetry of the molecule or ion in the crystal. This explains why the bending mode in crystalline KNCO is split whereas that of NaNCO is degenerate as predicted by the symmetry of the isolated cyanate ion.

In addition to the departure from the selection rules for the free molecule, crystals will exhibit lattice vibrations which, while of too low frequency to be readily observed as a fundamental, will in many cases be observable in combination with the molecular vibrations. A number of otherwise unexplained subsidiary absorption peaks found in the vicinity of absorption bands due to

molecular vibrations have been attributed to such combinations. Newman and Halford (37, p. 1276-1290; 38, p. 1291-1294) for example have attributed a series of absorptions on both the high and low frequency sides of several bands in NH_4NO_3 and $TlNO_3$ to a series of combinations of the fundamental molecular vibrational modes with several lattice vibrational modes. The bands on the low frequency side are of course difference bands. As yet no rigorous rules have been found for determining the allowed infrared absorption bands in crystals. This stems in part from the difficulties caused by other factors which enter into the picture and complicate the situation enormously. Such other factors include librational motions and perturbations due to coupling with the vibrational modes of neighboring molecules and ions.

Walnut has shown that coupling between the vibrational motions of equal or nearly equal frequencies of neighboring molecules in crystals should give rise to a series of lines rather than a single absorption line. This series, however, will in most cases only give rise to a broadening of the absorption bands in crystals. J. C. Decius (14, p. 1290-1294) has made a quantitative treatment of the special cases of nitrate and carbonate

ions in lattices where the interionic coupling constant would be expected to be large. In these cases it has been shown that the coupling is sufficient to give rise to a series of bands which are sufficiently separated to allow some resolution of the bands.

Hexter and Dows (29, p. 504-509) have studied the effects of librational motion on the fundamental vibrations and have found evidence for the presence of combination bands between vibrational and librational modes in a few solids. They point out that in crystals transitions of the type $(v,n) \rightarrow (v+1,n)$; $(v,n) \rightarrow (v+1,n+1)$; $(v,n+1) \rightarrow (v+1,n)$; etc., where v is the vibrational quantum number and n is the librational quantum number, should give rise to O, P, Q, R, etc. branches to the fundamental vibration band in a manner similar to the corresponding P,Q,R branches found in gases. Since the librational frequencies are expected to be fairly low, the population of molecules in excited librational states should be rather high at room temperature and even at fairly low temperatures. For this reason all branches should have a structure of their own consisting of a different line for different values of n. Assuming this latter series of lines to be unresolved, one would expect each branch to shade to higher, or lower

frequencies depending on the anharmonicity effects of the librational motion. Since lattice modes are likewise of low frequency the foregoing discussion should apply to them also.

Some indication of the magnitude of these effects can be gained by observing the changes in the absorption bands due to changes in temperature and environment. Line broadening due to librational or vibrational motions and in fact any other effect related to the presence of the molecule in an excited state should be affected by changes in temperature. On the other hand line broadening due to coupling of the vibrations of neighboring ions should be affected by changing the vibrational frequencies of the neighboring ions either by isotopic substitution, or by actual replacement with different types of ions. In the solid solution technique used in this work both methods have been used to alter the interionic coupling. One particular advantage of the use of solid solutions is the ability to achieve nearly complete isolation of the ions from like ions by using sufficiently dilute solutions. It is, however, not possible to obtain solutions of very high concentration, the upper limit of concentration occurring around 2%.

2. Temperature Effects

A decrease in the temperature of a solid should be manifested in the spectrum in two different ways.

First the absorption bands would be expected to be sharpened. In the solid state the molecules or ions undergo thermal vibrations about their mean positions. This thermal agitation, which has an amplitude of about 0.03 Å (34, p. 362) from the mean position at room temperature, causes a statistical number of the ions to be in a potential field which is not well defined but rather covers a range equal to the range of the potential field over the region of space within which the molecule or ion moves. Because the molecular vibrational frequencies which give rise to infra-red absorption depend upon the potential field in which the molecule finds itself, it is clear that the more exactly defined this field is for all the molecules, the more exactly will the vibrational frequency be defined, and consequently the sharper the absorption lines will be. Thus as the temperature is lowered, the amplitude of thermal agitation decreases and the absorption lines will get sharper.

Secondly the equilibrium population of excited states will change with change of temperature so that the

intensity of absorption bands, especially for excited vibrational states, will change. According to the Boltzmann distribution law the equilibrium ratio of molecules in the two different energy states i and j is given by the equation

$$\frac{n_i}{n_j} = \frac{d_i}{d_j} \exp -(\epsilon_i - \epsilon_j)/kT$$

where n_i = the number of molecules with energy ϵ_i

d_i = the degeneracy of the energy state i

k = the Boltzmann constant

T = the temperature.

Table 3 gives the Boltzmann distribution ratios for a number of vibrationally excited states compared to the ground state at four different temperatures.

In addition to these expected temperature dependent effects, yet another effect of temperature may be observable. As the temperature is changed, the lattice dimensions will change slightly and might be likened to a compression of the lattice. Recently work has been done by Drickamer (45, p. 1226-1227) in which the infrared spectrum of cyanate (mistaken for cyanide) dissolved in alkali halide crystals was studied while subject to high pressures. A decrease in wavelength with increase in pressure was found.

Table 3

Ratios of the Number of Molecules in Excited Vibrational States to the Number of Molecules in the Ground State at Different Temperatures

ν (cm^{-1})	$e^{-\frac{\nu hc}{kT}}$			
	150°K	210°K	300°K	450°K
76	0.48	0.595	0.70	0.79
94	0.41	0.525	0.64	0.74
150	0.24	0.28	0.49	0.62
200	0.15	0.25	0.38	0.53
300	0.055	0.125	0.24	0.38
630	0.0024	0.0135	0.0488	0.135
630 (doubly degenerate)	0.005	0.027	0.10	0.27
1260	----	0.0002	0.0024	0.018
1260 (triply degenerate)	----	0.0006	0.0075	0.054
1890	----	----	0.000123	0.0024
1890 (quadruply degenerate)	----	----	0.00049	0.01
2170	----	----	----	0.001

The nature of the mechanism by which the lattice dimensions affect the vibration frequencies is not very well understood as yet. This topic will be briefly discussed in a later chapter.

III. EXPERIMENTAL METHODS

A. The Spectrometer

1. The Instruments

All spectra were obtained using a Perkin-Elmer Model 122 C infrared spectrometer which utilizes the Walsh double pass monochromator principle (51, p. 96-100). In order to obtain maximum dispersion, a number of different interchangeable prisms were used in the monochromator. The region from 500 to 700 cm^{-1} was covered using a KBr prism, that from 700 to 1950 cm^{-1} using a NaCl prism, while a LiF prism was used for higher frequencies. Since the instrument used is not a double-beam instrument, the presence of atmospheric water vapor and carbon dioxide made it very difficult to observe any weak bands which might occur in the region where these gases absorb strongly. For this reason it is quite possible that any absorption bands in these regions might be missed entirely or incorrectly measured. This difficulty was considerably reduced by flushing out the instrument with a steady stream of nitrogen gas, but this technique was not entirely successful. A cursory examination of the NaCl prism region was made in the later stages of the work on a recently acquired double beam instrument. This work

revealed no new absorption bands.

In the region from 3800 cm^{-1} to higher frequencies an instrument utilizing a quartz prism should give better dispersion. Consequently a Beckman Model DK-2 spectrophotometer was also used to observe bands in the short wave length region beyond 3800 cm^{-1}. Since this instrument was not calibrated, however, no wavelength measurements taken from it have been used.

2. Calibration

In order to obtain the greatest possible accuracy in the determination of the frequencies of the absorption peaks, a technique was devised which gave internal calibration points to all spectral records. This technique consisted of first making a calibration chart of the region in question. This calibration chart was made sufficiently large so that no additional errors were introduced due to inaccurate plotting and reading of the chart. The data used in making the calibration charts was the average of the results of a number of separate measurements, the number varying between three and fifteen with most charts being made from the data from about five separate runs. The sample was then placed in the path of the spectrometer beam and the region about the absorption band was scanned. After the absorption peak was passed,

the sample was removed and the appropriate calibration gas was placed in the beam. Thus without stopping the wavelength scanning mechanism the spectrum of the sample and the calibration gas were recorded on the same chart. The distance of the sample absorption peak from the calibration points could then be measured and the wavelength read off the calibration chart. The reported absorption peaks in this work are the average values obtained by repeating this process three to ten times. The experimental errors reported are derived from the scatter of the individual measurements about these average values with additional allowance for inaccuracies in the calibration chart.

The calibration charts were prepared using the gases and frequencies recommended by Downie et al. (18, p. 941-951). In the case of carbon monoxide gas used for calibration in the region from 2050 to 2225 cm^{-1} the more recent frequency measurements of Plyler, Blaine, and Connor (41, p. 102-106) were used.

For the region around 2700 to 2850 cm^{-1} it was noted that the frequencies referred to by Downie et al. were for HCl^{35} whereas the ordinary HCl gas used contains both HCl^{35} and HCl^{37}. The absorption peaks due to HCl^{37} fall approximately 2 cm^{-1} below those of HCl^{35}. In this

region the slit widths used on the spectrometer were about 2.2 cm^{-1} which is too wide to resolve the peaks due to each chlorine isotope and so the resulting absorption peak will lie between that expected for each isotope separately. David Dows (19, p. 73) has recently noted this difficulty and has recommended a correction of about -0.7 cm^{-1} to the frequencies quoted by Downie et al. for slit widths sufficiently large (3.0 cm^{-1} or greater). For slits of 2.2 cm^{-1} this correction would be somewhat reduced due to the partial resolution of the two peaks. In this work a correction factor of -0.4 cm^{-1} has been added to the frequencies for HCl as given by Downie et al.

3. Low and High Temperature Measurements

The low temperature spectra were obtained by placing the samples in a low temperature cell similar to that described by Wagner and Hornig (49, p. 297-298). The cell was then evacuated and the cold-finger was filled with liquid air, or a dry ice-acetone mixture. The cell was modified to accommodate a thermocouple which was in some cases attached to the sample and in other cases was sandwiched between the sample crystal and a rock salt window. Thus it would seem that the principal error in temperature measurement (that due to inadequate contact

with the sample) would result in temperature readings which are somewhat high. The thermocouple was checked at dry ice temperature and found to agree with the tables found in the Chem. Rubber Handbook to within 2°K so that in general the temperature measurements are assumed to be accurate to within ±8°K.

The high temperature cell consisted of a large brass plate heated with a nicrome wire coil. In the middle of this 3/4 inch thick plate was a hole in which the sample was held. The plate was surrounded with aluminum foil and a layer of asbestos but was otherwise exposed to the air. A thermometer well in the plate was used to determine the approximate temperature of the window. A thermocouple attached to the window being used to obtain an accurate relationship between the true sample temperature and the temperature recorded by the thermometer. The temperature was regulated by manual control of a variac which controlled the voltage applied to the heating coils.

B. Sample Preparation

In the study of the infrared spectrum of solids several techniques are commonly used in the preparation

of the sample. These techniques have been developed as a means of reducing the amount of light scattering and holding a measured and controlled amount of sample in the light path.

The most obvious way of reducing the amount of scattered light is by means of liquid solutions. Unfortunately such solutions usually are found to give rather broad absorption bands due to the variety of possible environments in which the sample molecules find themselves. In addition other rather complex and little understood effects are caused by solvation, or hydrogen bonding, or other such perturbations. Due to these difficulties of interpretation and other experimental difficulties, very little work was done with liquid solutions.

1. Nujol Mulls

A standard procedure for obtaining the infrared absorption spectrum of a solid is to form an emulsion. The most common liquid used is nujol as it absorbs only weakly in just a few regions. To form an acceptable mull, one which scatters very little radiation, the solid sample must be finely pulverized so that the particle size is small with respect to the wavelength of the infrared radiation being used. Usually the solid is ground

between two NaCl plates using the liquid as a carrier. The particles are generally considered sufficiently fine if the mull appears orange when viewed against a light. The resulting suspension is then evenly distributed between a pair of NaCl plates and the plates, called windows, are placed in the beam of the spectrometer.

Another technique used was that of placing a solution of the sample in 95% alcohol on NaCl or KBr windows and allowing it to evaporate. The evaporation was hastened by means of a heat lamp in order to prevent the growth of large crystals. Upon drying, more solution was added to the surface of the windows. This process was repeated until a sufficient amount of sample was deposited. Nujol was then added to reduce the amount of light scattering.

The latter technique is particularly useful when only a small amount of solid is available or when, as was the case in the preparation of $NaNC^{13}O$ and $KNC^{13}O$, the sample is provided in an alcoholic solution.

2. KBr Pressed Pellets

A more recently developed technique of preparing solid samples is the KBr pressed pellet technique (46, p. 1805). This consists of mixing the sample with some well dried KBr and grinding the mixture to a very fine

powder either in a mortar and pestle or in a ball mill. The powder is then placed in a specially constructed die and subjected to a pressure of 75,000 to 100,000 psi. At this pressure the KBr is formed into a clear disk. If the concentration of sample is kept sufficiently low, usually below 1%, the clarity of the KBr disk is not greatly impaired. There are a number of minor details which are helpful in producing clear disks. Most important are the use of dry KBr and sample, evacuating the die before and during the application of pressure, and the use of care in obtaining an even distribution of disk material in the die.

This technique has the advantage of utilizing all the sample material. In addition quantitative work can be done as the concentration of sample may be exactly known. The only disadvantage of the technique is the fact that the spectrum may actually be slightly altered due to gradual solution of the sample in the salt. Thus it has been shown (1, p. 1104) that repeated pressing and grinding of a 50-50 mixture of KBr and KCl results in the complete fusion of the two lattices after a total of ten cycles.

A similar disadvantage was found to be operative in the use of nujol mulls. Thus after mulling some samples of cyanate between NaCl windows the very sharp peaks of

cyanate dissolved in NaCl were found superimposed on the much more diffuse absorption band due to sodium cyanate. It was also found that potassium salts readily react with NaCl windows and become sodium salts. These difficulties may be due to a small amount of water in the nujol. This water might dissolve small amounts of both sample and window thus allowing exchange of ions between the two. The technique of depositing the sample by evaporation of an alcoholic solution was found to be particularly favorable to the exchange of ions between sample and window.

3. Solid Solutions

The principal development of this work was the use of the new technique of studying substances in solid solution. The use of solid solutions for small molecules or ions has the advantage over liquid solutions of restricting the possible positions of the sample with respect to neighboring molecules and ions. In fairly dilute solutions there is little or no possibility of like molecules being close enough together to perturb each other due to coupling between their vibrational modes. This results in spectra which are generally sharper than either pure solids or liquid solutions.

Unfortunately the best results are obtained from

growing single crystals with the sample dissolved in impurity amounts; this entails either growing from a melt or growing from solution. The latter is a very tedious process requiring a great deal of time, and consequently it requires that the sample be inert with respect to the solvent. Growing single crystals from a melt on the other hand requires high temperatures and thus severly limits the number of samples which may be studied.

In addition solid solutions may be formed by co-precipitation techniques and the resulting powder studied as a nujol mull or as a pressed pellet.

4. The Growth of Single Crystals

Due to the fact that there is a solid state group in the chemistry department working under the direction of Prof. A. B. Scott, the technique of growing alkali halide single crystals was very easily acquired.

There has been considerable work devoted to the growth of large single crystals and the literature contains a number of different methods (10, p. 1-571). The method used here is that commonly referred to as the Kyropoulos method, although it departs in many respects from the technique devised by Kyropoulos (36, p. 308-313;

35, p. 849-854).

a. Kyropoulos Method

This method consists of first melting the alkali halide in a crucible placed in a small furnace. A seed crystal is then inserted into the melt through a hole in the roof of the furnace and slowly pulled out. As the seed crystal is withdrawn from the melt the melt tends to crystallize out on it thus causing the crystal to grow. This crystal growth requires both that the melt be just a few degrees above the melting point and that the seed be cooled by some mechanism.

The crystal growing apparatus was essentially the same as that described by W. Fredericks (21, p. 16-19) except for the following modifications.

The placement of the thermocouple as used in Fredericks' apparatus was found to be very critical and rather difficult to reproduce, consequently the temperature of the oven was estimated and regulated by means of an ammeter and variac. The current necessary to maintain the oven at the proper temperature remained nearly constant over a large number of runs so that with a very small amount of practice it was possible to estimate the proper setting for the variac to maintain the furnace at the proper temperature.

In an average run the alkali halide was placed in a porcelain crucible and melted in the furnace. The cyanate was not introduced until ready to grow the crystal as it was found to decompose within about twenty minutes. After all was ready, the desired amount of cyanate was poured into the molted salt and the seed crystal inserted as soon as the cyanate was completely dissolved. In many cases cyanide was used in place of cyanate; the oxidation to cyanate takes place almost immediately.

As the seed crystal was slowly withdrawn the solution was observed to give off a few bubbles due to the decomposition of the cyanate (which is discussed below). An induction period of about ten to fifteen minutes during which few bubbles were observed allowed sufficient time to grow a small crystal nearly completely free of bubbles. After this initial period the production of gas bubbles increased rapidly thus frustrating most attempts at the growth of large crystals. Besides impairing the optical properties of the crystals, the presence of a large number of bubbles promoted the growth of multiple crystals and eventually caused the growth of a completely randomly oriented crystal mass. Finally after about thirty minutes all the cyanate was found to have decomposed as crystals grown from the solution heated for a

half-hour were found to contain no cyanate but plenty of carbonate and nitrite.

b. Bridgman Method

In order to grow a crystal containing cyanide it was necessary to remove the possibility of reaction of the cyanide with oxygen in the air. This was achieved by growing the crystal in an evacuated Vycor capsule. In this instance the crystal was grown by the Bridgman method which consists of lowering the capsule through a furnace. The bottom of the capsule was constricted into a capillary in order to increase the probability of obtaining a single crystal. At an undetermined time a thin portion of the capsule imploded, but the weak cyanate absorption and strong absorption in the region expected from the cyanide indicate a reasonable degree of success in preventing the complete oxidation of the cyanide. Although the crystal was not a single crystal as indicated by difficulty in cleaving, a clear portion was obtained large enough to obtain a good spectrum.

C. High Temperature Chemistry of Cyanate Ion

The first alkali halide crystals containing cyanate ion were grown in a platinum crucible as it was expected

that this would produce fewer impurities than porcelain crucibles which probably add impurities due to the slow solution of the glaze. Because of the prolific formation of gas bubbles the production of single crystals was difficult to achieve and even in the best specimens it was difficult to find nearly bubble free volumes of a useable size.

Although very little high temperature chemistry has been done on cyanate, Hofmann et al. (30, p. 204-212) found a metal catalyzed oxidation of KNCO takes place in air at a temperature of 400°C, damp air giving a greater rate than dry air, and the metal catalytic activity increasing through the series Cu < Ni < Ag. In as much as platinum is generally considered an excellent catalyst for many reactions catalyzed by nickel or silver, it is logical to deduce that the decomposition observed in growing crystals in a platinum crucible could be minimized by the use of some other material such as porcelain. This surmise was borne out by experiment. Since the glaze in porcelain crucibles also contains some heavy metals one might expect the reaction to slow down considerably, but not to cease entirely. Using the evolution of gas bubbles as a gauge of reaction rate, this prediction was verified.

Hofmann et al. hypothesize the break down of cyanate

with water vapor to form carbonate and ammonia gas. The latter reacts further to form nitrate. These workers also hypothesize a different, slower reaction with forms nitrate directly.

Another reaction which cyanate undergoes is the reduction to cyanide at high temperatures. According to Portevin (43, p. 308-310) this reaction should be important at the temperatures obtaining in the melt. However, since our work was carried out in air, the partial pressure of oxygen was quite large. Our experience shows that the oxidation reaction is still far more important at the temperature of the molten salts. In fact that oxidation reaction was utilized in most of the work as a convenient means of forming cyanate.

5. Preparation of Samples Containing Carbon-13.

A sample of KCN containing 61.9 atom percent carbon-13 obtained from Eastman Kodak was used as raw material for making all samples of cyanate substituted with carbon-13.

Initially the samples of $KNC^{13}O$ were prepared by oxidation of the cyanide with lead dioxide at elevated temperatures. The resulting cyanate was then dissolved in water or alcohol. Most frequently an alcoholic solution was made as it was found possible to evaporate

this directly on the KBr windows as described on pages 54-57.

All samples of $NaNC^{13}O$ and one of $KNC^{13}O$ were prepared by adding cyanogen chloride to an alcoholic solution of the appropriate hydroxide, i.e.

$$ClCN + 2NaOH \xrightarrow{alc.} NaCl + NaNCO + H_2O$$

This method quite naturally favored the coprecipitation of NaNCO in NaCl and consequently gave rise to a small amount of solid solution.

The ClCN was prepared by a method described by Cook and Robinson (13, p. 1001-1005) modified so as to remove excess Cl_2 by evaporation into a stream of nitrogen gas.

The solid solutions were formed by merely introducing $KC^{13}N$ to the melt instead of KNCO. Oxidation in air was found to be very nearly complete within a few seconds.

6. Possible Impurities

According to the discussion on high temperature chemistry one would expect in the alkali halide solutions to find infrared absorption bands due to the various decomposition products of cyanate ion. Consequently care must be exercised to look for absorption bands due to

carbonate, cyanide, nitrate, and nitrite ions. The nitrite is a further decomposition product due to the reduction of nitrate which readily takes place at high temperatures. The literature contains a wealth of information regarding the infrared spectrum of these possible impurities. In addition a crystal of each of these ions dissolved in KBr was grown and the resulting spectra summarized in Tables 4, 5 and 6. The presence of carbonate and nitrite ions was detected in most crystals grown, but in all crystals used the impurities were of such low concentration that only the stronger fundamentals were observed.

In the spectrum of sodium cyanate and potassium cyanate it is only necessary to worry about impurities due to hydrolysis of the cyanate. Carbonate is again a very important product while ammonium ion and bicarbonate are other possible products, neither of which were observed to give any absorption bands in any of the spectra. The presence of cyanide was also considered, but no evidence for it was found.

Table 4

Infrared Spectrum of Nitrite Ion Dissolved in KBr

Frequency (cm^{-1})	Intensity	Width
2760	medium	sharp
2550	medium	broad
2425	medium	sharp
2095	weak	medium
1375	very strong	broad (due to intensity)
1270	very strong	broad (due to intensity)
840.5	medium	sharp

Table 5

Infrared Spectrum of Carbonate Ion Dissolved in KBr

Frequency (cm^{-1})	Intensity	Width
1460	medium	sharp to medium
1414	very strong	medium
1156	medium	broad
1138	medium	broad
883	medium	sharp

Table 6

Infrared Spectrum of Potassium Cyanide
Dissolved in KBr

Frequency (cm^{-1})	Intensity	Width
1952.2	weak	sharp
1961.0	medium	sharp
2029.8	medium	sharp
2070.4	very strong	broad with sharp maximum

IV. EXPERIMENTAL RESULTS

A. Assignments

Table 7 contains a list of observed infra-red absorption frequencies for a potassium bromide single crystal containing a small amount of potassium cyanate. Figures 2 through 5 contain a plot of percent transmission vs. frequency (wave number) to show the shape and strength of the absorption bands. Similar data for other alkali halide salts and pure cyanate salts are contained in Tables 9, 10, 12, 16, and 17 and Figures 8, 9, 10, 11 and 12. Since the spectrum of cyanate ion is changed but little on going from pure cyanate to a solid solution in alkali halide, only the assignments for the absorption bands in KBr will be discussed in detail. In addition a few important differences due to change of crystal lattice will be discussed separately for each crystal.

Assuming a linear structure for the cyanate ion one expects to find three fundamental vibrational frequencies due to the normal modes of vibration shown in Figure 1. Thus only three strong absorption bands are expected whereas four are found. From the expected magnitude of the force constants for a C-N triple bond

Table 7

Observed Infrared Spectrum of Cyanate Ion in Potassium Bromide*

Assignment		Frequency (cm^{-1})	Assignment		Frequency (cm^{-1})
$\nu_2' \rightarrow \nu_1$		574.4	ν_3	N^{15}	2152.5
$\nu_2' \rightarrow 2\nu_2^\circ$		663.2	ν_3	O^{18}	2161.5
$\nu_2' \rightarrow \nu_1$	C^{13}	578.7	$2\nu_1$		2392.9
$\nu_2' \rightarrow 2\nu_2^\circ$	C^{13}	659.1	$\nu_1 + 2\nu_2^\circ$		2487.25
			$4\nu_2^\circ$		2602.5
ν_2'		629.4			
ν_2'	C^{13}	612.0	$2\nu_1$	C^{13}	2360.3
			$\nu_1 + 2\nu_2^\circ$	C^{13}	2462.6
ν_1		1205.5	$4\nu_2^\circ$	C^{13}	2554.2
$2\nu_2^\circ$		1292.6			
$\nu_2' \rightarrow \nu_1 + \nu_2'$		1188.1	$\nu_2' \rightarrow 2\nu_1 + \nu_2'$		---
$\nu_2' \rightarrow 3\nu_2'$		1309.1	$\nu_2' \rightarrow \nu_1 + 3\nu_2'$		---
			$\nu_2' \rightarrow 5\nu_2'$		2628.25
$2\nu_2^2 \rightarrow \nu_1 + 2\nu_2^2$		1175.5			
$2\nu_2^2 \rightarrow 4\nu_2^2$		1320.4	$\nu_2' + \nu_3$		2788.1
			$\nu_2' \rightarrow 2\nu_2^2 + \nu_3$		2776.55
ν_1	O^{18}	1175.8			
$2\nu_2^\circ$	O^{18} or NO_2^-?	1260.1	$\nu_2' + \nu_3$	C^{13}	2714.0
ν_1	N^{15}	1188.9	$\nu_2' \rightarrow \nu_1 + \nu_3$		2725
$2\nu_2^\circ$	N^{15}	1282.3	$\nu_2' \rightarrow 2\nu_2^\circ + \nu_3$		2813
ν_1	C^{13}	1191.0	$\nu_1 + \nu_3$		3355.0
$2\nu_2^\circ$	C^{13}	1272.5	$2\nu_2^\circ + \nu_3$		3442.2
$\nu_2' \rightarrow \nu_1 + \nu_2'$	C^{13}	1174.4	$\nu_2' \rightarrow 3\nu_2' + \nu_3$		3325.7
$\nu_2' \rightarrow 3\nu_2'$	C^{13}	1285.7	$\nu_2' \rightarrow \nu_1 + \nu_2' + \nu_3$		---
ν_3		2169.6	$2\nu_2^\circ + \nu_3$	C^{13}	3284.1
$\nu_2' \rightarrow \nu_2' + \nu_3$		2158.55	$\nu_1 + \nu_3$	C^{13}	3366.0
$2\nu_2^2 \rightarrow 2\nu_2^2 + \nu_3$		2147.9			
			$\nu_2' \rightarrow 3\nu_2' + \nu_3$	C^{13}	3257.2
ν_3	$N^{15}C^{13}O$	2094.6	$\nu_2' \rightarrow \nu_1 + \nu_2' + \nu_3$	C^{13}	---
ν_3	$NC^{13}O^{18}$	2104.8			
			$\nu_1 + \nu_3$	N^{15}	3322.0
ν_3	$NC^{13}O$	2112.8	$2\nu_2^\circ + \nu_3$	N^{15}	3414.7
$\nu_2' \rightarrow \nu_2' + \nu_3$	$NC^{13}O$	2102.2			

Table 7 - Cont.

Assignment	Frequency (cm^{-1})
$2\nu_1 + \nu_3$	4524.7
$\nu_1 + 2\nu_2^\circ + \nu_3$	4623.0
$4\nu_2^\circ + \nu_3$	4737.5

* Table 10 gives additional frequencies for the fine structure in the region from 2000 to 2390 cm^{-1}.

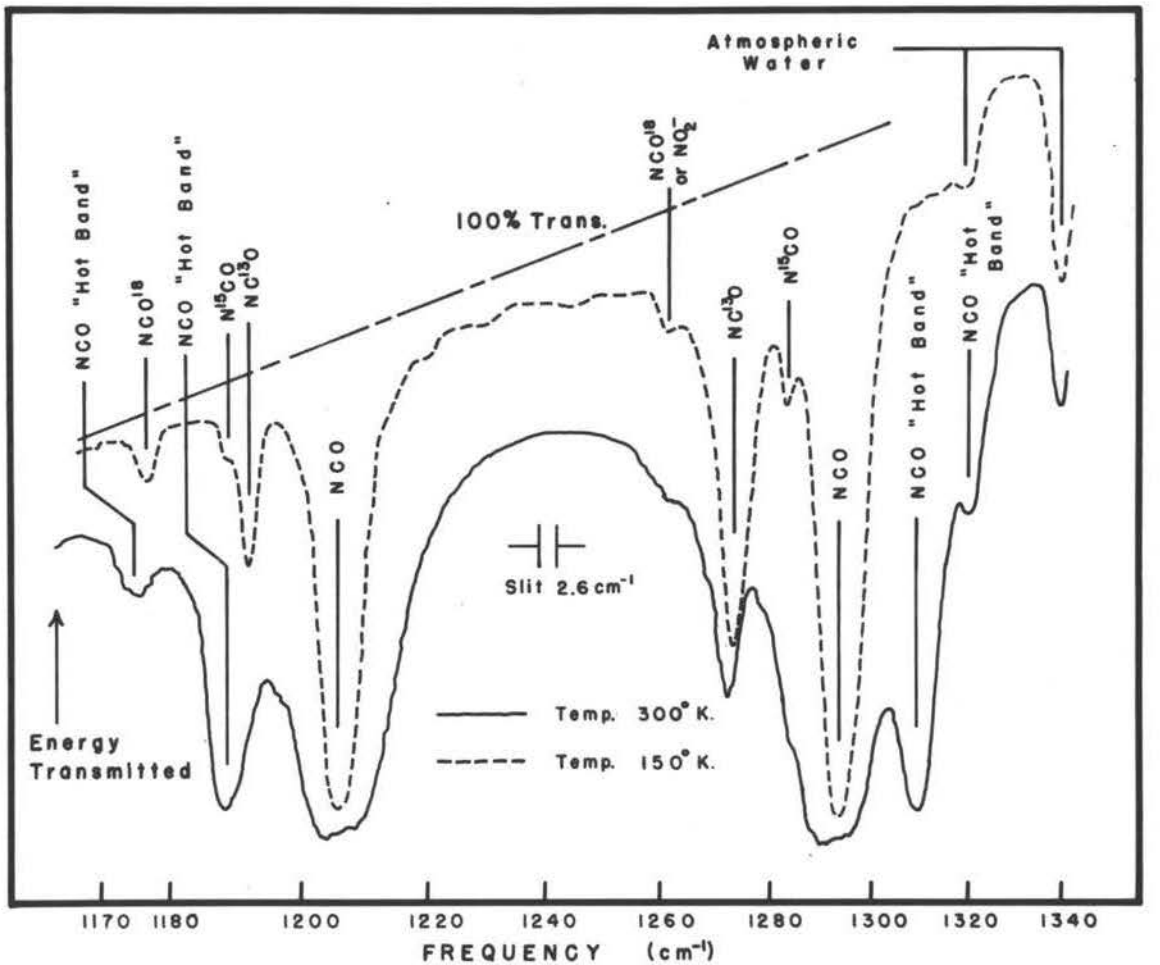

FIGURE 2

SPECTRUM of CYANATE in KBr HOST in SYMMETRIC STRETCH REGION

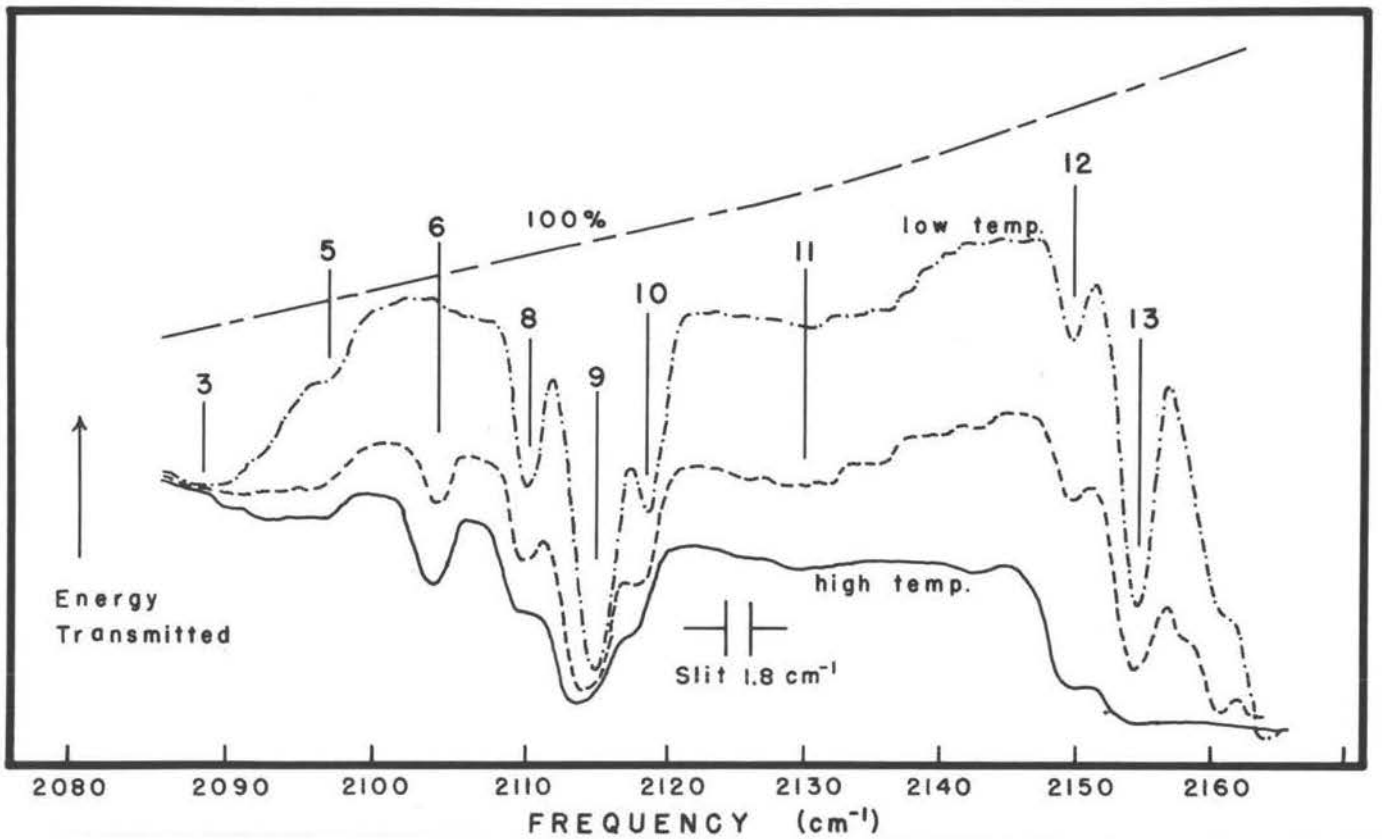

FIGURE 3

INFRARED SPECTRUM of CYANATE ION in KBr LATTICE as CRYSTAL IS WARMED from LIQUID AIR TEMPERATURE to that of DRY ICE

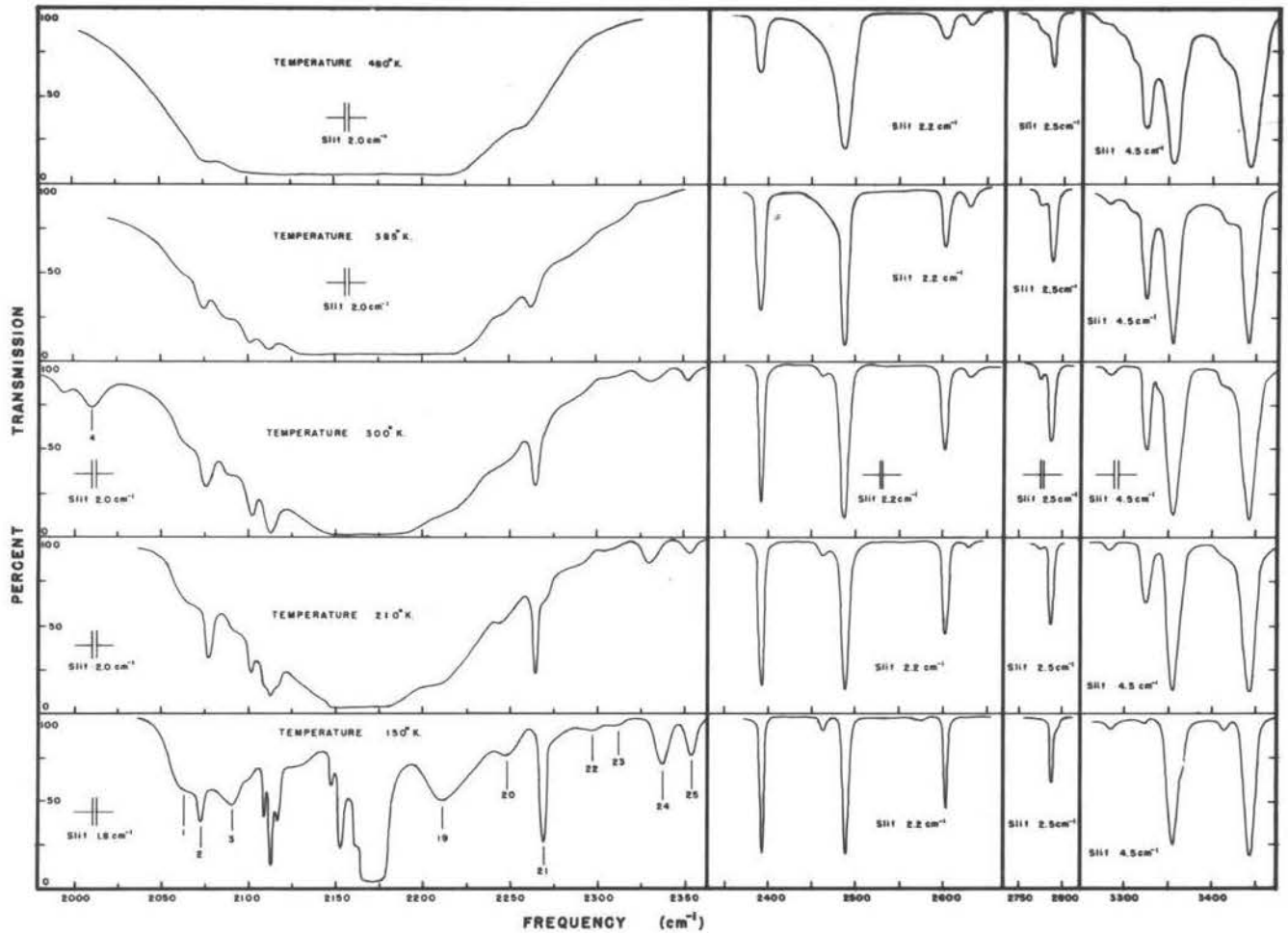

FIGURE 4

INFRARED ABSORPTION SPECTRUM of CYANATE ION in KBr HOST LATTICE
at DIFFERENT TEMPERATURES

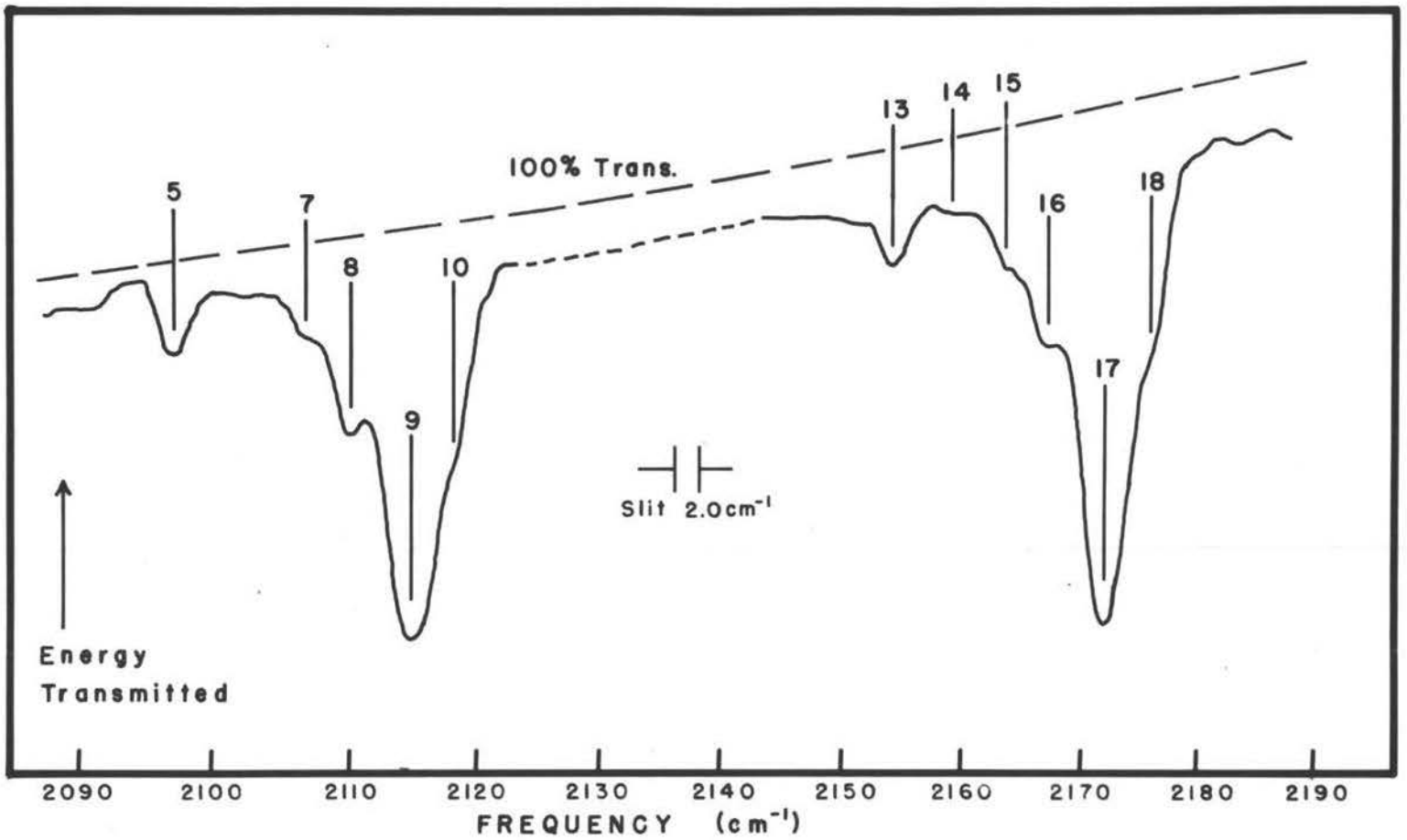

FIGURE 5

INFRARED ABSORPTION of CYANATE CONTAINING 61.9% C^{13} at 150°K.

and a C-O double bond it is expected that ν_3 should lie around 2200 cm^{-1}, ν_1 around 1200 cm^{-1}, and ν_2 around 600 cm^{-1}. Thus one is led to the assignment of the 2169.6 cm^{-1} band to the asymmetric stretching vibration which is mostly a C-N stretching vibration and the 629.4 cm^{-1} band to the bending vibration ν_2. The presence of two bands of very nearly equal strength at 1205.5 and 1292.6 cm^{-1} is explained as due to Fermi resonance between ν_1 and the first overtone of the bending frequency, $2\nu_2^{\circ}$. This resonance, if the coupling is great enough, causes each vibration to contribute a portion of its character to the other so that for strong resonance the two lines will be equal in intensity and contain equal contributions from the two resonating vibrations.

Another effect of the resonance between $2\nu_2^{\circ}$ and ν_1 is the increase in separation of the two frequencies, the lower one being lowered by a certain amount and the upper frequency being raised by the same amount. As shown in Appendix II, the coupling constant for the Fermi resonance of excited vibrational states is larger, consequently the weaker peaks at 1188.1 and 1309.1 cm^{-1}, again of nearly equal intensities, are considered to be due to the transitions $\nu_2' \rightarrow 3\nu_2'$ and $\nu_2' \rightarrow \nu_1 + \nu_2'$. The additional separation of these two peaks is approximately

equal to that predicted by theory. The two quite weak peaks at 1175.5 and 1320.4 cm^{-1} are similarly assigned to the transitions $2\nu_2^2 \rightarrow 4\nu_2^2$ and $2\nu_2^2 \rightarrow \nu_1 + 2\nu_2^2$. If these assignments are correct the latter two pairs of resonating peaks should be very temperature dependent. Sure enough, as the temperature of the crystal is lowered to about dry ice temperature the peaks due to a lower state of $2\nu_2^2$ disappear and those assigned to ν_2^1 as lower state diminish considerably in intensity. Upon reducing the temperature to around 150°K the peaks at 1188.1 and 1309.1 disappear altogether as expected. Table 3 shows the expected abundance of molecules in the various excited states at different temperatures. It is evident that at 150°K the only vibrational states which might be excited in an appreciable amount would be those of low frequency such as lattice modes.

Of the weaker peaks which must be due to overtones or combination bands, two peaks at 3355.0 and 3442.2 cm^{-1} are assigned to the combinations of the Fermi resonant vibrations with the asymmetric stretch. These of course give two bands of nearly equal intensity. In thicker samples one might expect to observe weaker bands both higher and lower than these two which would correspond to "hot bands" with a lower state containing one quantum

of bending vibrational energy (ν_2^1), however, due to the negative anharmonicity constants these two resonating hot bands ought to be displaced a few wave numbers lower. One such band has been observed at 3325.7 cm^{-1} while the other is almost certainly obscured by the strong peak at 3442.2 cm^{-1}. Repeated efforts to resolve this weak peak have been fruitless. The predicted frequency of this peak further supports the supposition that it is close enough to the strong peak to be beyond the resolution capabilities of the monochromator. Further support for the assignment for the peak at 3325.7 cm^{-1} is afforded by the fact that it disappears at liquid air temperatures as predicted.

At 574.4 and 663.2 cm^{-1} are found two more temperature dependent peaks which have been assigned as transitions from ν_2^1 to $2\nu_2^\circ$ and ν_1 . These peaks when added to the observed bending fundamental ought to be exactly equal to the frequencies of the two Fermi resonant peaks due to $2\nu_2^\circ$ and ν_1 . This has been found to be true within experimental error.

At room temperature a series of nearly equally spaced lines appears below the ν_3 fundamental. These satellites diminish in intensity as they become further removed from the fundamental and their intensities are

strongly temperature dependent. They too have been attributed to "hot bands" in which the ground state of the ion has one, two, etc. quanta of bending motion. An indication of the validity of this assignment is afforded by the observation of a peak at 2788.1 cm^{-1} which has been assigned to the combination band and consequently should be exactly equal to the sum of ν_2' and the first hot band for ν_3. Actually the deviation of 0.3 cm^{-1} is considered very good agreement. In the same region around 2700 cm^{-1} one might expect to find absorptions due to the transition $\nu_2' \rightarrow 2\nu_2^2 + \nu_3$, $\nu_2' \rightarrow 2\nu_2^\circ + \nu_3$, $\nu_2' \rightarrow \nu_1 + \nu_3$. These very weak peaks have in fact been found at 2776.55, 2813, and 2725 cm^{-1} respectively. The temperature dependence of the latter two could not be observed due to their extreme weakness; however, the peak at 2776.55 cm^{-1} has been observed to disappear as the sample is cooled with liquid air.

There yet remain two triplets which are assigned as Fermi resonant triplets due to $2\nu_1$, $\nu_1 + 2\nu_2^\circ$, $4\nu_2^\circ$ at 2392.9, 2487.25, and 2602.5 cm^{-1} and $2\nu_1 + \nu_3$, $\nu_1 + 2\nu_2^\circ + \nu_3$, $4\nu_2^\circ + \nu_3$ at 4524.7, 4623.0, and 4737.5 cm^{-1}. These assignments lead to predicted positions which are quite close to the actually observed values. In addition a temperature dependent peak has been found

at 2628.25 cm^{-1} which is believed due to a hot band for the highest line of the resonant triplet $2\nu_1 + \nu_2'$, $\nu_1 + 3\nu_2'$, $5\nu_2'$.

In the region around the very strongly absorbing ν_3 band there are a number of subsidiary bands which are believed due to various crystal type motions. These peaks will later be discussed in detail for each crystal.

Because some of the samples contained a large amount of cyanate ion, it is expected that some absorptions due to the natural abundance of molecules containing isotopes such as C^{13} and N^{15} ought to be observed. The observation of excited states for which populations are calculated to be below 1% also indicates that the more common isotopically substituted ions ought to be observable. Comparison of the observed spectrum of $N^{14}C^{12}O^{16}$ with that of $N^{14}C^{13}O^{16}$ prepared from isotopically enriched cyanide shows that some weaker peaks are due to different isotopic species in their natural abundance. The use of liquid air to sharpen the absorption and thus remove overlapping with the stronger $N^{14}C^{12}O^{16}$ peaks has revealed even more absorptions due to isotopes. Thus for the strongest fundamental it is possible to see absorptions due to the C-N stretching fundamental for the six isotopically different ions $N^{14}C^{13}O^{18}$, $N^{15}C^{13}O^{16}$, $N^{14}C^{12}O^{16}$,

$N^{15}C^{12}O^{16}$, $N^{14}C^{13}O^{16}$, and $N^{14}C^{12}O^{18}$. The Force constants for the cyanate ion may be used to test these assignments as shown in Table 8. Included in Table 7 are the absorption bands assigned to various naturally abundant isotopic species.

B. Sodium Cyanate

Figure 6 shows the form of the infrared absorption spectrum of pure sodium cyanate. Only the fundamental bands are shown here as the overtones were too weak and broad to be very easily observed. The exceptional strength and broadness of the 2225 cm^{-1} band make it difficult to assign a definite frequency to this vibrational mode. This coupled with the Fermi resonance perturbation for the symmetric stretching mode around 1250 cm^{-1} render any calculations of the stretching force constants too unreliable to be of value, consequently only the bending force constant for the cyanate ion has been calculated and tabulated in Table 9 along with the frequencies of the normal and C^{13} containing ion. It will be noted that the Redlich-Teller product rule is obeyed as well as can be expected. The same figure shows the absorption spectrum for cyanate enriched with 61.9% C^{13}. It is curious that the asymmetric stretching band

Table 8

Comparison of Observed and Calculated Frequencies for Various Isotopic Species in KBr

Observed freq. (cm^{-1})	Calculated[a] freq. (cm^{-1})	Calculated[b] freq. (cm^{-1})
	$N^{14}C^{12}O^{16}$	
574.4	576.1	576.1
663.2	663.2	663.2
629.4	629.4*	629.4*
1205.5	1205.5*	1205.5*
1292.6	1292.6*	1292.6*
1188.1	c 1186.2	1188.1*
1309.1	1310.9	1309.1*
1175.5	1170.1	1174.65
1320.4	1326.1	1321.55
2147.9	2147.5	2147.5
2158.55	2158.55*	2158.55*
2169.6	2169.6*	2169.6*
2392.9	2390.6	c 2395.1
2487.25	c 2484.7	2484.4
2602.5	2607.2	2603.0
----	2354.6	
----	2487.8	
2628.25	2637.3	2628.8
2788.1	2787.95[d]	2787.95[d]
2776.55	2776.40[d]	2776.4[d]
2725	2725.6	2725.6
2813	2812.8	2812.8
3355.0	3355.0*	3355.0*
3442.2	3442.2*	3442.2*

Table 8 - Cont.

Observed freq. (cm^{-1})		Calculated[a] freq. (cm^{-1})		Calculated[b] freq. (cm^{-1})
3325.7		3324.3		3326.2
----		3449.8		3447.9
4524.7		4519.1		
4623.0		4615.5		
4737.5		4736.4		
		$N^{14}C^{13}O^{16}$		
578.7				
659.1				
612.0		612.0*		612.0*
1191.0	c	1190.3	c	1190.3
1272.5		1271.8		1271.8
1174.4		1172.0	c	1175.1
1285.7		1289.5		1286.4
2102.2		2102.3		2102.3
2112.8		2112.8*		2112.8*
2360.3		2355.8		
2462.6		2462.5		
2554.2		2557.0		
2714.0		2714.3		2714.3
3284.1		3283.1		3283.1
3366.0		3366.1		3366.1
3257.2		3254.3		3257.3
----		3373.3		3370.3

Table 8 - Cont.

Observed freq. (cm^{-1})	Calculated[a] freq. (cm^{-1})	Calculated freq. from force constants (cm^{-1})
	$N^{15}C^{12}O^{16}$	
----	626.1	626.1
1188.9	c {1190.1	c {1190.5
1282.3	{1283.5	{1283.9
2152.5	2152.5*	2151.3
3322.0	{3323.0	
3414.7	{3416.1	
	$N^{14}C^{12}O^{18}$	
----	624.8	624.8
1175.8	{1175.8*	{1175.8*
1260.1 ?	{1274.4	{1273.4
2161.5	2161.5*	2163.5

* Frequencies used to calculate the potential constants

[a] Calculations were made using the single Fermi resonance constant B; braces connect Fermi resonant levels

[b] Calculations were made using the two Fermi resonance constants a and b; braces connect Fermi resonant levels

[c] Calculations were based upon the sum of these Fermi resonant peaks

[d] Calculations were based upon the difference of these two frequencies

FIGURE 6

INFRARED SPECTRUM of SODIUM CYANATE

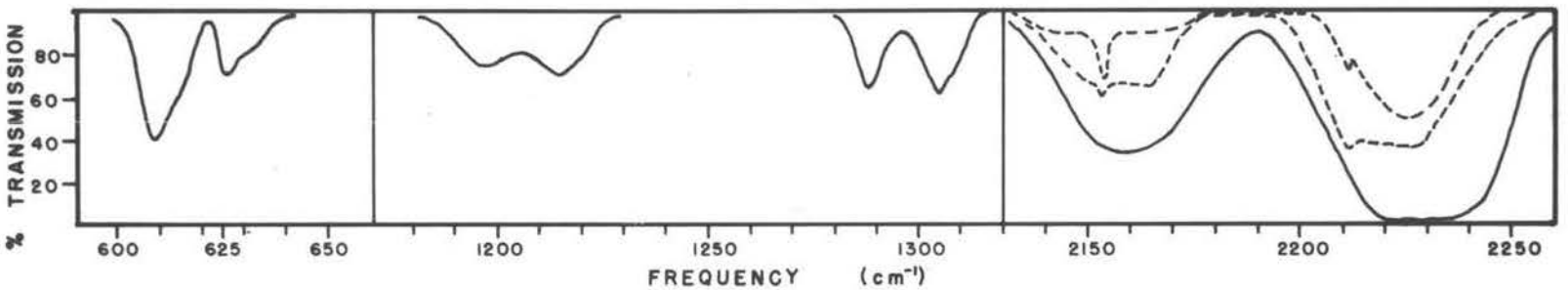

NaNCO Containing 61.9 Mole % $NaNC^{13}O$

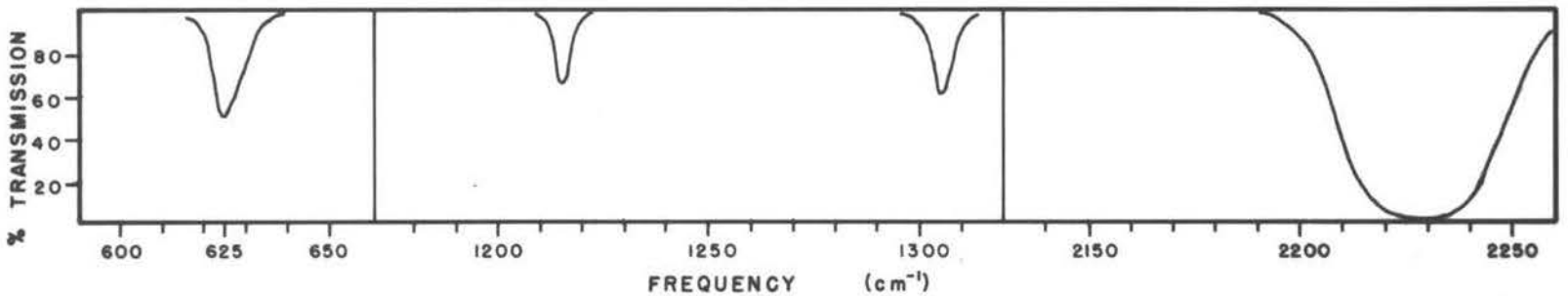

NaNCO Containing 1.1 Mole % $NaNC^{13}O$

Table 9

Infrared Fundamentals and Constants
for Sodium and Potassium Cyanate

Assignment	NaNCO Freq. (cm^{-1})	$NaNC^{13}O$	KNCO Freq. (cm^{-1})	$KNC^{13}O$
ν_1	1214.5	1197.2	1207.3	1194.6
$2\nu_2$	1304.5	1288.0	1301.5	1277.0
ν_2	624.3	608.7	628.0	612.3
ν_2			636.9	620.0
ν_3	2226	2160	2165	2111.5

Bending Force Constants

	$k_\alpha / l_1 l_2$	k_α
NaNCO	0.491 md/Å	0.706 md Å/radian
$NaNC^{13}O$	0.493 md/Å	0.710 md Å/radian
KNCO	0.511 md/Å	0.735 md Å/radian
	0.496 md/Å	0.714 md Å/radian
$KNC^{13}O$	0.512 md/Å	0.737 md Å/radian
	0.499 md/Å	0.719 md Å/radian

Assumed Bond Distances

NaNCO	C-N	=	1.17 Å
	C-O	=	1.23 Å
KNCO	C-N	=	1.17 Å
	C-O	=	1.23 Å

Table 9 - Cont.

Redlich-Teller Product for Bending Mode

Theoretical	1.02868
NaNCO	1.0256
KNCO	1.0264

for the C^{13} containing ion seems to be weaker than for the C^{12} ion. This same effect was noted in the case of pure KNCO. Both the method of preparing $NaNC^{13}O$ from $KC^{13}N$ and the method of preparing the sample for scanning the spectrum presented an opportunity for some of the cyanate to become trapped in the lattice of some NaCl. This accounts for the anomalously sharp peaks sometimes found superimposed on the otherwise normal spectrum as indicated by the dashed lines in Figure 7.

C. Potassium Cyanate

The most striking feature which differentiates the potassium cyanate infrared spectrum from that of sodium cyanate is the splitting of the degeneracy of the bending vibration. Upon studying the crystal structure of the two salts the reason for the difference in the two spectra becomes immediately apparent. M. Bassiere (9, p. 1309-1311) has found that sodium cyanate crystallizes in a hexagonal lattice in which the cyanate ions all lie parallel and along the axis of highest symmetry. Hendricks and Pauling (26, p. 2912-2916) have found that the crystal structure of KNCO is orthorhombic with the cyanate ions lying in parallel planes within which each ion is perpendicular to its nearest neighbor cyanate ion.

FIGURE 7

INFRARED SPECTRUM of POTASSIUM CYANATE

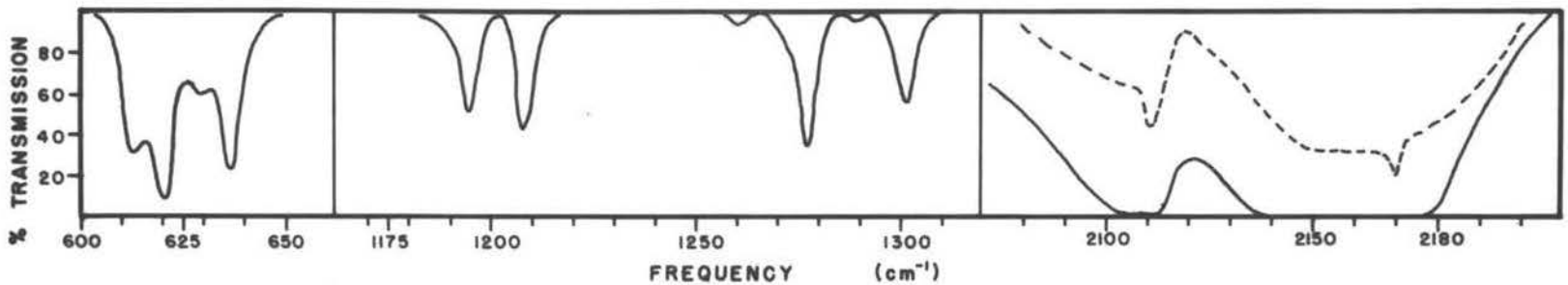

KNCO Containing 61.9 Mole % $KNC^{13}O$

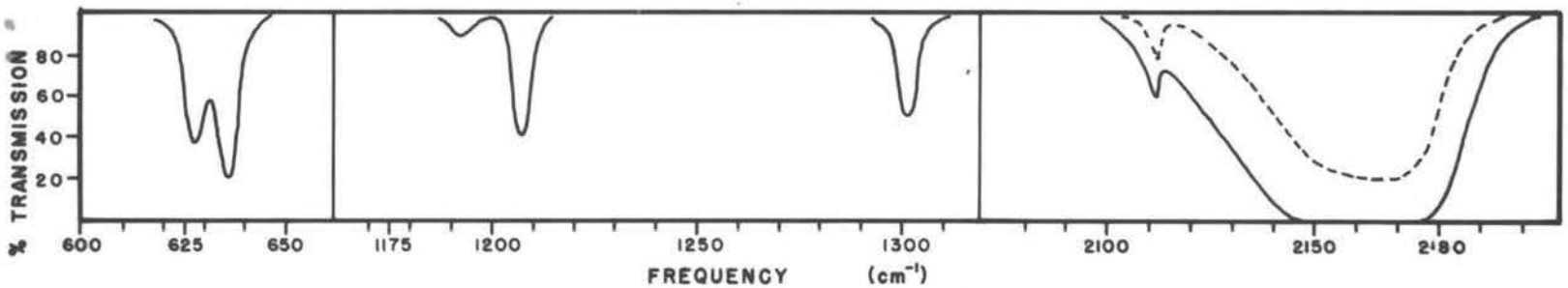

KNCO Containing 1.1 Mole % $KNC^{13}O$

Consequently the in-plane bending modes will have a different energy from the out-of-plane bending modes thus splitting the otherwise degenerate bending mode. In-as-much as the ions are closer within the plane and therefore more likely to encounter more resistance to vibration, the higher frequency absorption is expected to be the in-plane bending motion while the lower absorption frequency is probably the out-of-plane bending mode. It is interesting to note that both frequencies are above that found for the sodium salt. The lower of the KNCO bending frequencies is very nearly the same frequency found for the alkali halide solutions and hence indicates that this vibration is very likely subject to little or no external influences. The sodium cyanate bending mode on the other hand has an unusually low frequency and may be subject to interionic coupling effects which would tend to lower the frequency. This coupling is much more likely in sodium cyanate due to the fact that the ions are all lined up with their axes parallel, whereas the cyanate ions in the KNCO lattice are all perpendicular and so the bending modes should be nearly completely uncoupled. L. Jones (32, p. 1069-1072; 33, 1234-1236) has found a similar splitting of the bending mode for the thiocyanate ion in KNCS for which the crystal structure is similar to that of KNCO.

In most mulls of the potassium salt a sharp peak was found which coincided with the frequency of $NC^{13}O$ and consequently appears to be due to this ion in isolation among $NC^{12}O$ ions which perturb it only slightly and hence lead to a sharp peak in contrast to the broad peak due to the far more numerous carbon-12 containing ions. It is strange that this has not been observed in the case of sodium cyanate. The sharp peaks in the carbon-13 enriched spectrum are probably due to a potassium bromide solid solution of cyanate similar to that in the sodium cyanate enriched samples.

D. Solid Solutions

The principle assignments for the infrared spectrum of cyanate dissolved in solid alkali halides are essentially the same as that given for KBr as discussed above. It is found, however, that all vibrations are displaced to lower frequencies for KI and to higher frequencies for KCl and NaCl. The following paragraphs will give a description of the other absorption bands found in the various solid solutions and explain the origins of those peaks for which a ready explanation is forthcoming. After all the information is presented for

all the different solutions, the last part of this section will be devoted to a discussion of the various possible explanations for those absorption bands which remain.

1. KBr

At 612.0 cm^{-1} is a weak absorption which has been attributed to cyanate ions containing carbon-13. This assignment has been checked with a sample enriched in carbon-13. Also at 1191.0 and 1272.5 cm^{-1} are two bands which have been assigned to the same isotopic species. The lower of these two bands is obscured by a "hot band" at room temperature, but is quite prominent at liquid air temperatures. Also found in this same region for crystals containing a large amount of cyanate ions are four other peaks which show up at about -150°C (see Fig. 2). These peaks are considerably weaker than the C^{13} peaks and have been attributed to $N^{15}CO$ and NCO^{18} ions. All these frequencies and their assignments are given in Table 7. Five more peaks which coincide with the frequencies of C^{13} containing cyanate ions have been observed in thick crystals at 2102.2, 2112.8, 2463, 2554, and 3284 cm^{-1}. There are also four more peaks at 2152.5, 2161.5, 3283.8, and 3414.7 which are believed due to $N^{15}CO$ and NCO^{18}.

Figures 3 and 4 show the appearance of the transmission curve for cyanate in KBr at various temperatures.

Table 10 lists the frequencies of the peaks designated by numbers. Peaks No. 5, 6, 7, 9, 13, 14, 15, and 17 have already been mentioned as being due to "hot bands" or fundamentals for various isotopic species. The remainder are probably due to lattice vibrations and librations.

The broad absorptions No. 1 and 3 may be partly due to some cyanide ion impurities as cyanide dissolved in KBr has a broad absorption at about that position. In addition band No. 3 could correspond to a difference band for which the combination band is No. 20 at about 2248 cm^{-1}. Similarly No. 11 might correspond to the difference band for which No. 19 is the corresponding sum band. Other broad absorptions appear to be present at 22 and 23 and perhaps one which is obscured by the strong peak No. 21. Unfortunately the presence of a strong CO_2 absorption peak from the atmosphere greatly obscures the area from about 2300 to 2390 cm^{-1}. Within this region there are two absorption bands 24 and 25 which appear to be fairly sharp and more intense than 22 or 23. The peak at about 2353 cm^{-1} is very close to a peak due to C^{13} and may be due to the natural abundance of this isotope although it appears to be much too strong for this. The corresponding peak in a thin sample containing 62% C^{13} was distinguishable only with extreme difficulty. At

Table 10

Frequencies of Fine Structure Absorptions for Cyanate Ions Dissolved in KBr

Band Identity (see Figures 2, 3, and 4)	Frequency (cm^{-1}) at room temp.	Assignment
1	2065	cyanide
2	2078	difference band for lattice mode
3	2090	cyanide
4	2010	
5	2094.6	$N^{15}C^{13}O^{16}$ - ν_3
6	2102.2	$N^{14}C^{13}O^{16}$ - $\nu_2' \rightarrow \nu_2' + \nu_3$
7	2104.8	$N^{14}C^{13}O^{18}$ - ν_3
8	2108.3	
9	2112.8	$N^{14}C^{13}O^{16}$ - ν_3
10	2116.4	
11	2128	
12	2147.7	
13	2152.52	$N^{15}C^{12}O^{16}$ - ν_3
14	2158.55	$N^{14}C^{12}O^{16}$ - $\nu_2' \rightarrow \nu_2' + \nu_3$
15	2161.5	$N^{14}C^{12}O^{18}$ - ν_3
16	2164.9	
17	2169.60	$N^{14}C^{12}O^{16}$ - ν_3
18	2173.34	
19	2210	
20	2248	
21	2264	sum band for lattice mode
22	2296	
23	2307	
24	2336	
25	2353	

93.7 cm^{-1} below the fundamental is a sharp peak, No. 2, which is interpreted as a difference band. The corresponding sum band appears at 93.6 cm^{-1} above the fundamental and is likewise sharp and intense. Further support for this sum and difference assignment is afforded by the observation that at reduced temperatures both peaks become slightly more separated from the fundamental; the low frequency peak becomes slightly lower and the high frequency peak becomes slightly higher.

Of all the fine structure observable in the region about the asymmetric stretching fundamental, the presence of lines No. 8, 10, 12, 16, and 18 poses the greatest problem. These lines are as sharp as the nearest fundamental and approximately a fourth as intense although the exact ratio of intensities is difficult to ascertain. Table 11 tabulates the separation of these lines from the fundamental to which they seem related for all isotopic species and all solid solutions for which they have been observed. Different crystals of cyanate dissolved in KBr seem to give the same separation and intensity ratios for these bands, but the resolution appears to differ. It may be that the band width is a function of concentration. The most dilute crystals giving the best resolution. Temperature is of course important but does not seem to

Table 11

Separation of Satellite Absorption Bands
from the C-N Fundamental

Crystal	Ion	Frequency differences in cm^{-1}		
		Lower band	Upper band	Still higher band
KCl	$N^{14}C^{12}O^{16}$	3.75	4.65	
KBr	$N^{14}C^{13}O^{16}$	4.54	3.62	
KBr	$N^{15}C^{12}O^{16}$	4.80		
KBr	$N^{14}C^{12}O^{16}$	4.72	3.74	
KI	$N^{14}C^{13}O^{16}$	none resolved	2.86	
KI	$N^{15}C^{12}O^{16}$	none resolved	3.2	
KI	$N^{14}C^{12}O^{16}$			9.10

be the only factor. It will be noticed that the satellite bands are not equally separated from the fundamental. For the case of KBr solutions there seems to be an increase in the separation of the satellite peaks from the fundamental as one goes to lighter isotopes. The apparent reverse in going from $N^{15}CO$ to $N^{14}CO$ may be only experimental error. It would be interesting to find out if higher resolution work, use of thicker samples, and/or lowering the temperature still further might reveal similar subsidiary peaks alongside all other absorption bands. Since these peaks are not symmetrically placed about the fundamental, it is possible that for incompletely resolved peaks these satellite peaks will introduce errors in the apparent position of the main peak. Another experiment which should be performed is to see if the ratio of the intensities of these peaks is changed by change of temperature. If due to "hot bands" of any kind, the intensities of these peaks should decrease with decreasing temperature and the rate of decrease would allow an estimate of the frequency of the vibration involved.

2. KI

In the main the spectrum of KI solutions of KNCO is identical with that of KBr solutions except for the

slight decrease in frequency of all peaks. The magnitude of this frequency shift depends upon the nature of the vibration as the bending modes shift by only a few wave numbers whereas the C-N stretching mode is shifted by better than ten wave numbers.

Since no crystals were obtained containing as much cyanate as in the case of KBr solutions, not as many of the weaker absorption peaks were found as for KBr, but those which were found have corresponding absorption bands in KBr. The only apparent exceptions are in the region around the C-N stretching fundamental. Here again a wealth of fine structure has been resolved. Figs. 8 and 9 show the absorption bands in this region for the same crystal under conditions in every way identical except for temperature. Fig. 10 shows some of the same peaks on an expanded scale and under conditions of somewhat higher resolution. Table 12 gives the frequencies of the peaks for this region. Some of the observed peaks are readily assignable to "hot bands" or to fundamental absorptions due to the isotopic species $N^{14}C^{13}O^{16}$, $N^{15}C^{12}O^{16}$, and $N^{14}C^{12}O^{18}$ thus peaks C, D, F, G, H, J, and K can be accounted for.

The two diffuse and weak absorption bands designated as M and N in Figures 8 and 9 seem to correspond to the

Table 12

Fine Structure Frequencies for KI-KNCO Solutions

Identity (see fig. 5, 6, and 7)	Frequency (cm^{-1}) corrected to room temp.	Assignment	
A	2073.37	2080.07*	lattice difference absorptions
B	2077.94		
C	2088.4	$\nu_2' \rightarrow \nu_2' + \nu_3$	$(N^{14}C^{13}O^{16})$
D	2099.05	ν_3	$(N^{14}C^{13}O^{16})$
E	2101.91		
(not shown in figures)	2127.5	$\nu_2' \rightarrow \nu_2' + \nu_3$	$(N^{15}C^{12}O^{16})$
F	2134.2	$2\nu_2^2 \rightarrow 2\nu_2^2 + \nu_3$	$(N^{14}C^{12}O^{16})$
G	2138.70	ν_3	$(N^{15}C^{12}O^{16})$
V	2141.9		
H	2144.70	$\nu_2' \rightarrow \nu_2' + \nu_3$	$(N^{14}C^{12}O^{16})$
J	2148.15	ν_3	$(N^{14}C^{12}O^{18})$
K	2155.80	ν_3	$(N^{14}C^{12}O^{16})$
L	2164.90		
M	2184		
N	2214		
O	2233.7	2229.9*	lattice sum absorptions
P	2237.8		

Table 12 - Cont.

Identity (see fig. 5, 6, and 7)	Frequency (cm^{-1}) corrected to room temp.	Assignment
Q	2258.8	2266.3*
R	2274.3	
S	2289.4	
T	2308.3	

* Actual room temperature absorptions peaks

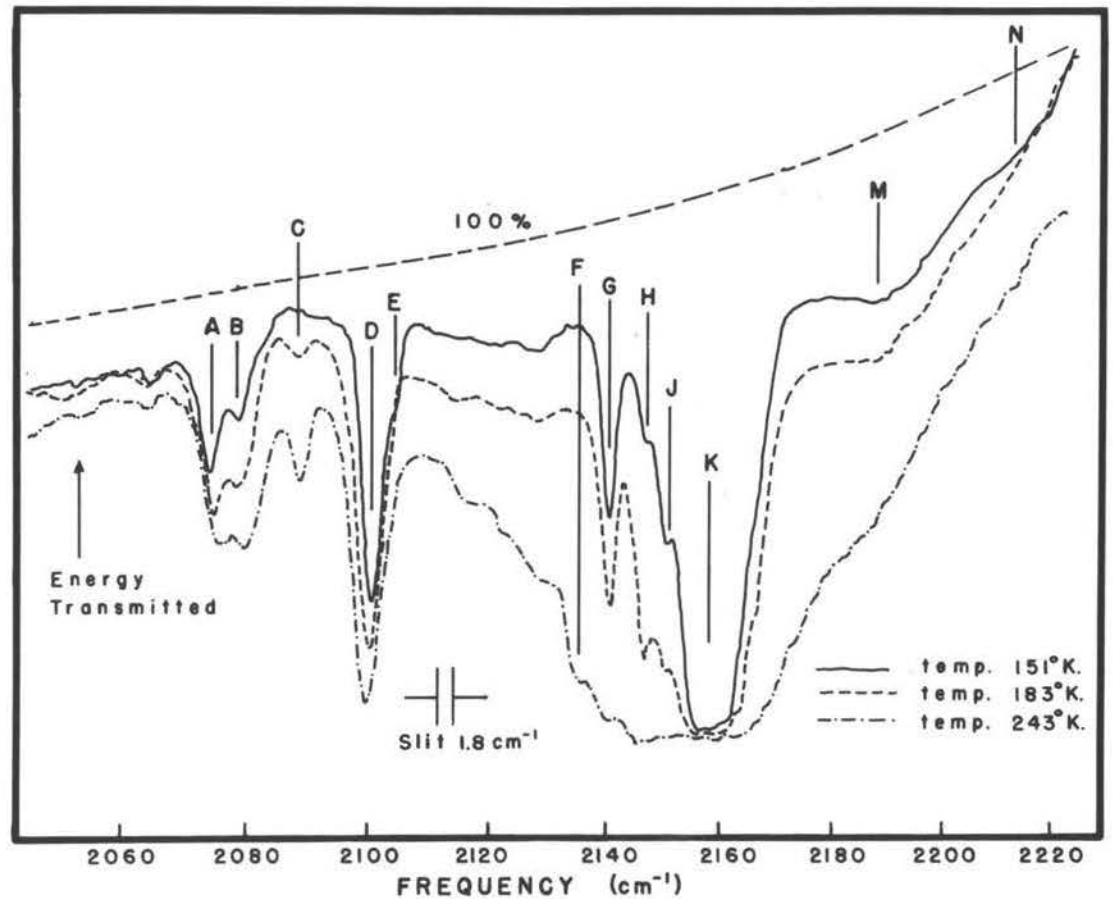

Figure 8

INFRARED ABSORPTION of CYANATE ION in KI LATTICE in REGION from 2060 to 2220 CM^{-1}

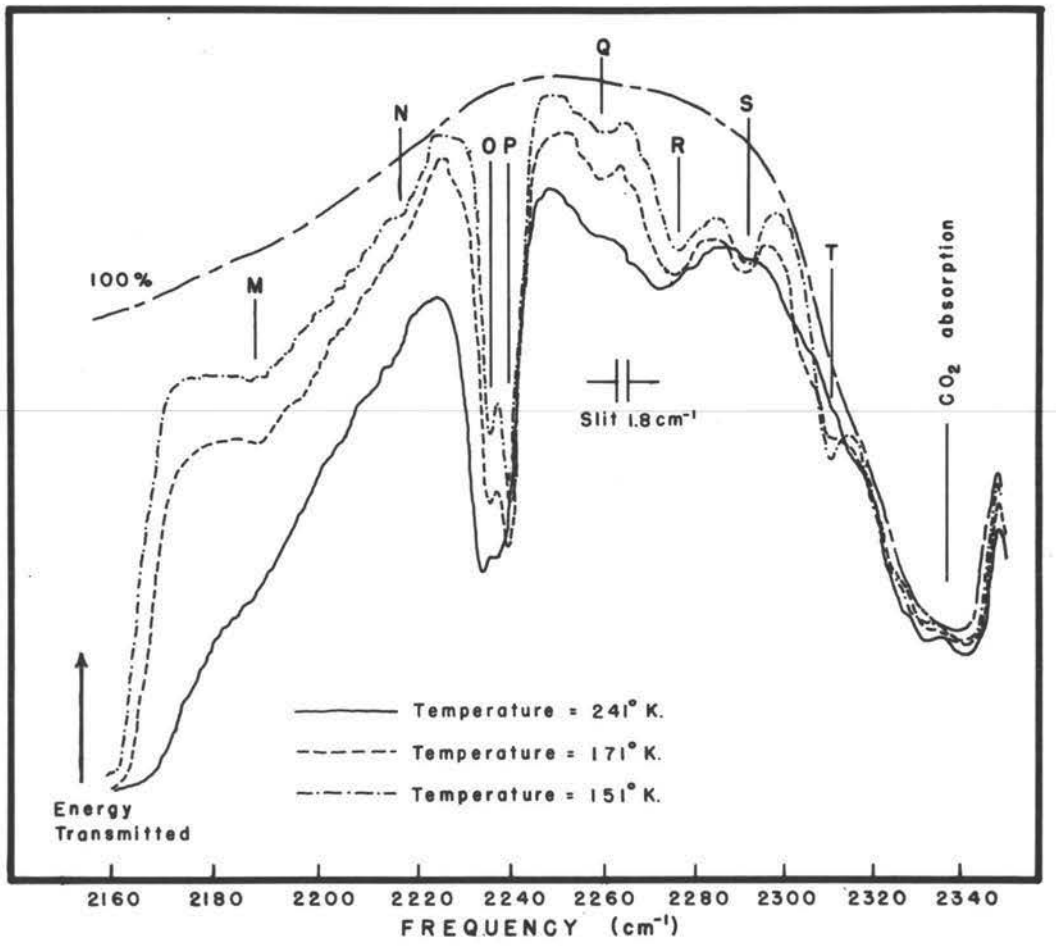

FIGURE 9

SPECTRUM of CYANATE in KI HOST LATTICE in REGION of ASYMMETRIC STRETCHING FREQUENCY from 2160 to 2340 CM^{-1}

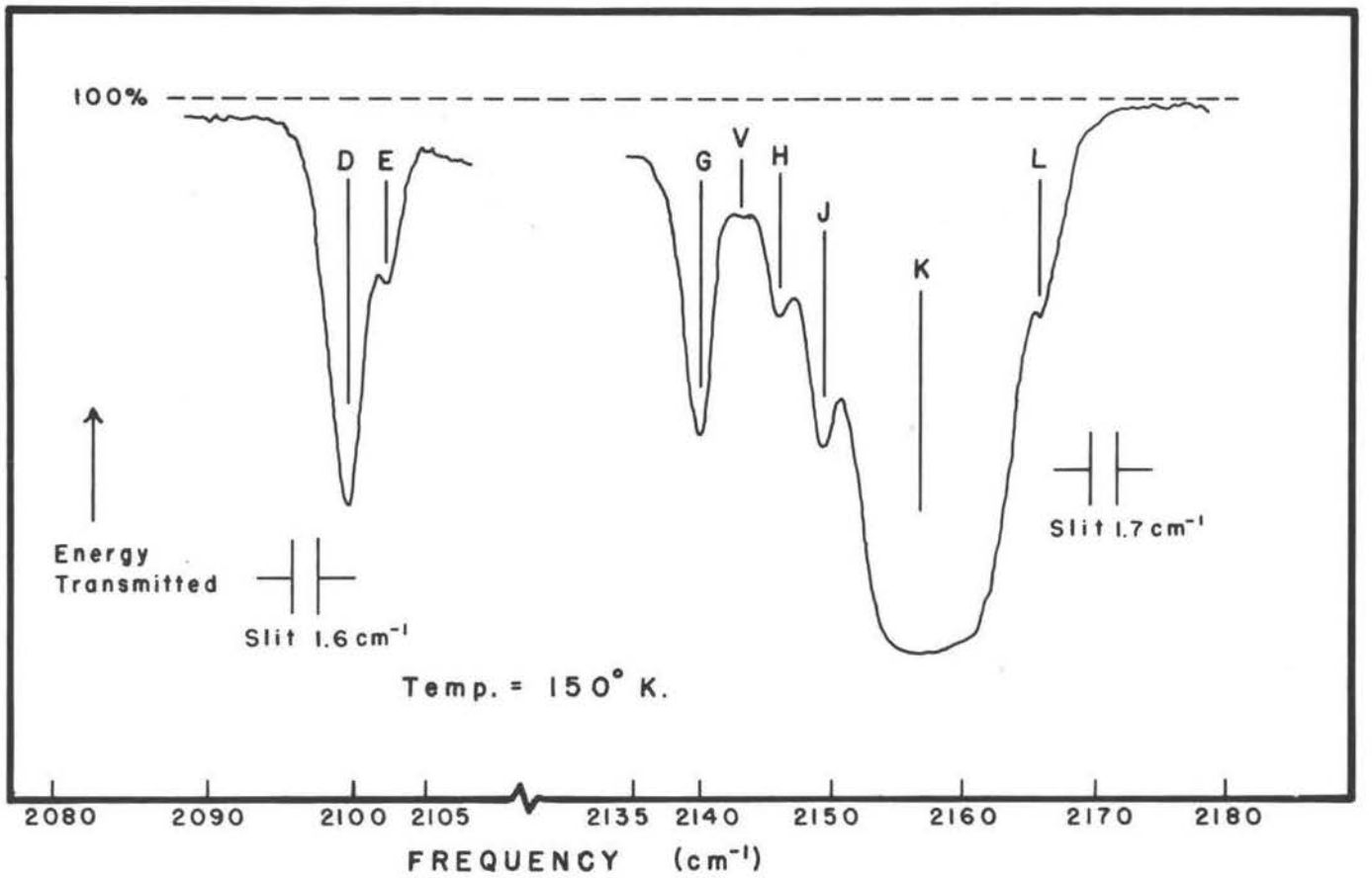

Figure 10

HIGHEST RESOLUTION INFRARED SPECTRUM of CYANATE ION in KI LATTICE in ASYMMETRIC STRETCHING REGION at LIQUID AIR TEMP.

bands No. 19 and 20 in KBr. At almost exactly 77.8 cm^{-1} above and below the fundamental band are found the two sharp rather strong absorption bands B and O. Next to these are a similar pair of intense sharp bands at 82.2 cm^{-1} above and below the fundamental. The figures show that at low temperatures the bands A and P are more intense than B and O whereas the ratio of intensities reverses as the temperature is increased until at room temperature the peaks B and O are the more intense. In addition the intensity of the pair A, B seems to increase with temperature whereas the sum of the intensities of O and P seems to remain nearly constant.

Above the high frequency doublet O and P is a series of nearly equally spaced bands Q, R, S, and T. These lines are broader and weaker than bands A, B and O, P but not as much so as M and N thus indicating some fundamental difference between the origins of these three sets of absorption bands. It is possible that there are more weak bands above T but the presence of a strong background absorption due to atmospheric CO_2 prevented observation of any weak peaks in this region. At room temperature these four or more bands are completely smeared out so that the only visible absorption is a broad band with a maximum absorption at the position of R.

In the case of KI there seem to be at least two and perhaps more satellites which accompany each fundamental for the C-N stretching vibration. Figure 10 shows the peaks E and L and possibly one for the $N^{15}CO$ band at V. Peak E is observed at about 2.9 cm^{-1} above the fundamental for $NC^{13}O$ whereas L is observed at 9.1 cm^{-1} above the $N^{14}C^{12}O^{16}$ fundamental. The thickness of the crystal used prevented observing any peaks closer to the fundamental for the most abundant ion, but it is expected that thinner samples would show a band corresponding to E around 3 cm^{-1} above the main peak. It is quite possible that we really have a series of equally spaced lines of rapidly diminishing intensity so that another line at ca. 6 cm^{-1} above the fundamental might be found in crystals containing the right concentration of cyanate. By analogy with the case of KBr and KCl solutions (see below) a peak below the fundamental might be expected. It is quite possible that one does occur, but is too close to the stronger fundamental to be resolved. This would mean that this peak is considerably less than 2.9 cm^{-1} from the fundamental, otherwise it would be resolved like E. Even more likely is the explanation that the satellite peaks found above and below the fundamental in KBr and KCl are displaced to higher frequencies in KI so that they

both appear above the fundamental.

3. KCl

No large crystals of KCl were prepared so that only a few features could be studied near the asymmetric stretching band. Figures 11 and 12 show that the usual "hot bands" and isotopic fundamentals are resolved and in addition two satellite absorptions above and below the strong $N^{14}C^{12}O^{16}$ fundamental. Although unsymmetrically located about the central strong peak as in KBr, it is here the high frequency peak which is separated from the main peak more than the low frequency peak while the reverse is true for KBr. There are also two weak, diffuse bands similar to M and N in KI. The lower peak which is like M in KI has a maximum absorption at about 2229 cm^{-1}. The absorption assigned to NCO^{18} seems anomalously strong in the thicker sample but in the thin sample shown in Fig. 11 the intensity appears about equal to that of $N^{15}CO$ as expected from the natural abundance of the isotopes.

4. NaCl

Only the most intense absorptions of a solid solution of cyanate in NaCl have been observed. All vibrations are displaced to rather high frequencies in

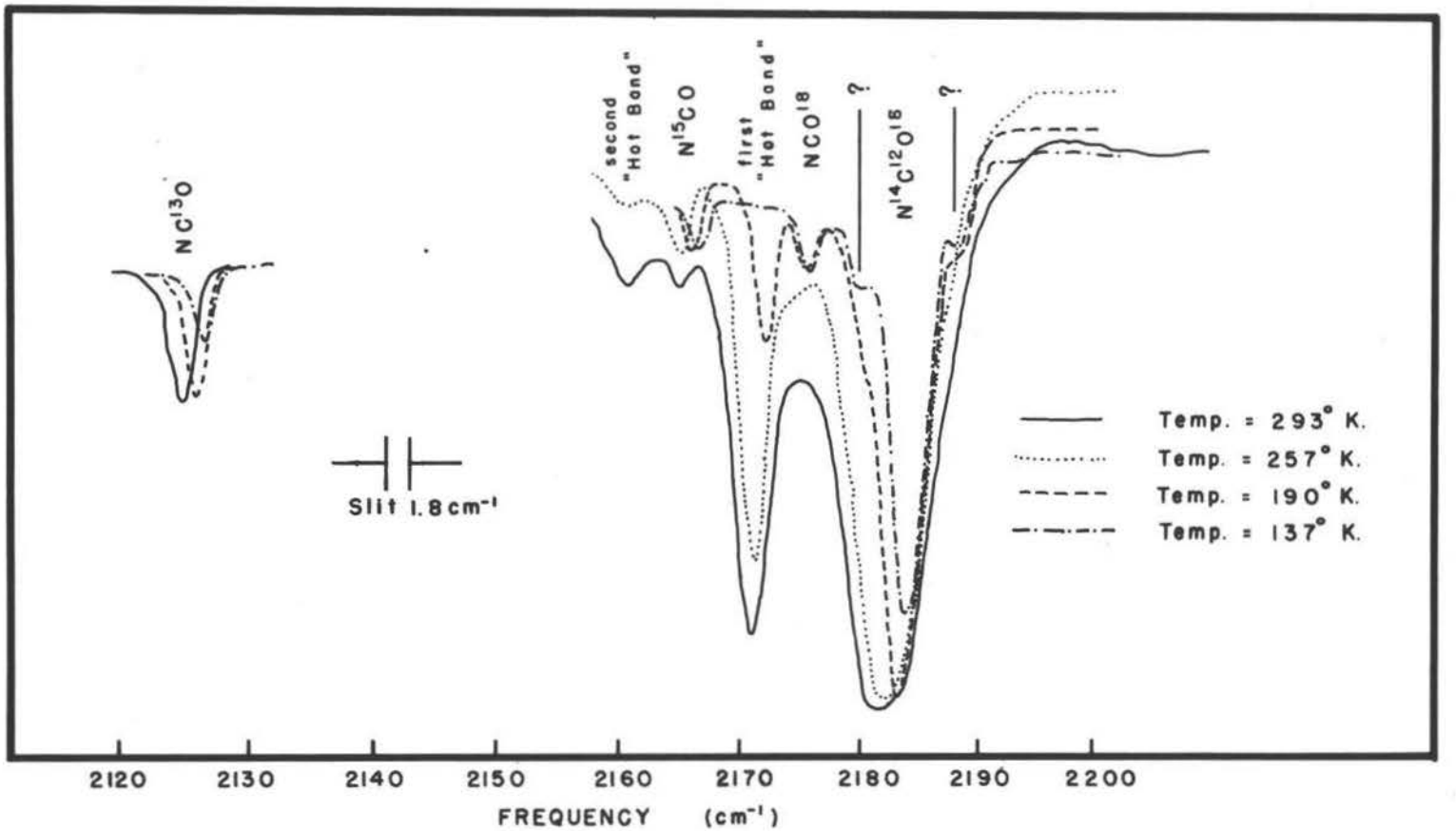

FIGURE II

INFRARED ABSORPTION of CYANATE ION in KCl LATTICE at DIFFERENT TEMPERATURES

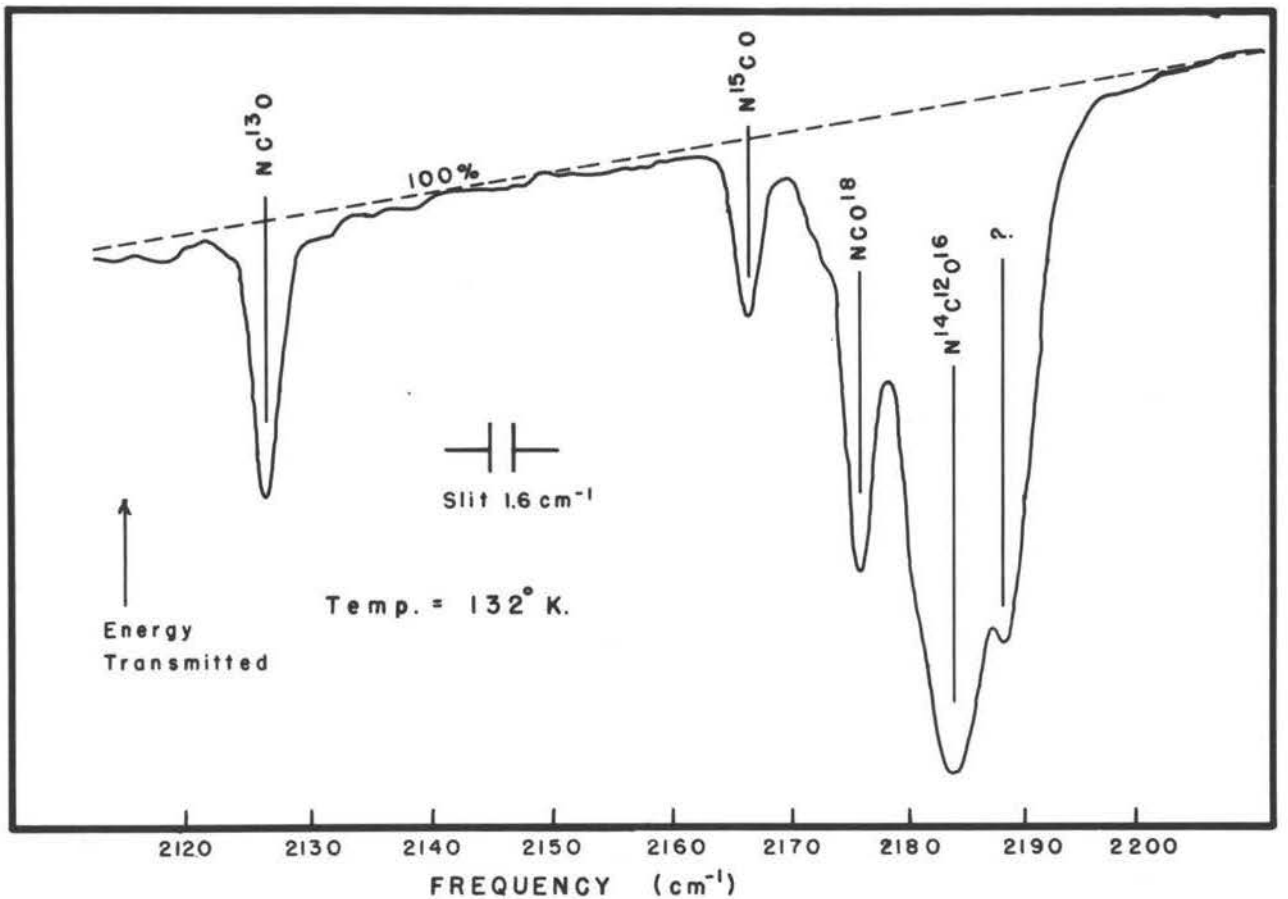

FIGURE 12

INFRARED ABSORPTION of CYANATE ION in KCl HOST LATTICE in ASYMMETRIC STRETCHING REGION at LIQUID AIR TEMPERATURE

line with the fact that the lattice dimensions of NaCl are smaller than those of any other lattice studied.

E. Fine Structure Assignments for the C-N Stretching Region

It is expected that any cyanate ions present at imperfections in the crystal will not give rise to sharp absorption bands merely because there will be a great many different ways in which the ions can be oriented at an imperfection so that in dealing with large statistical numbers of ions all possible orientations will be represented and as each will give rise to a slightly different frequency the total absorption will form a broad band. On the other hand when the cyanate ions merely replace a halide ion in the lattice, assuming this can be done without distorting the lattice too much, then each ion will be in the same environment and hence will give rise to rather sharp absorptions. If one further assumes that all cyanate ions are oriented so that the axis of the linear ion is directed along a body diagonal of the unit cell cube, then one expects to get very sharp lines. For this reason only the more diffuse absorption bands are suspect as being due to ions at imperfections. As stated above there are two classes of diffuse absorptions.

Taking KI as an example the peaks in one class are those designated by the letters M and N, and those in the other class are Q, R, S, and T. In KCl the peak corresponding to M is found to have a maximum at around 2229 cm^{-1}. A recent work by Drickamer (45, p. 1226-1227) in which KCl pellets are made from a melt to which KCN is added (a process which will lead to oxidation of the CN^- to NCO^-) has found an absorption peak at 2232 cm^{-1} in addition to the main fundamental at 2182 cm^{-1}. Drickamer presents evidence which indicates that this absorption is due to the cyanate ion at imperfection sites while the 2182 cm^{-1} peak is due to the cyanate ion at normal negative ion positions within the lattice. Since the peak which has here been observed at 2229 cm^{-1} is rather weak and diffuse, it seems reasonable to assume that it is the 2232 cm^{-1} peak observed by Drickamer. Furthermore, Drickamer observed the peak to disappear upon annealing of the pellets. In the process of growing single crystals the crystals are cooled slowly and so are already annealed. This would explain the very low intensity of the band in this work. It would, of course, be expected that there will always be a few imperfections which will never be annealed out. Now, if the peak corresponding to M is due to cyanate at an imperfection site, the weaker band at N

may well be due to cyanate ions at a different type of imperfection site. In KBr this same idea may be used to explain peaks 19, 20 and perhaps the weaker peaks 22 and 23. This means that there is no sum and difference relation connecting 1, 3, and 11 with 19, 20 and the others. Either 1 and 3 are due solely to cyanide in the crystal (a likely explanation) or they may be due to other types of imperfection sites (not so likely) or there is some other explanation.

There are several possible explanations for the presence of the satellite peaks which accompany each fundamental C-N stretching vibration. The possibility that these peaks are P and R branches due to the free rotation of the cyanate ion is easily eliminated as a freely rotating molecule would give greater P and R branch separations. Another possibility is suggested by the likelihood of hindered rotation for which the potential function has several equivalent minima. As in the case of inversion of the ammonia molecule such a multiple minimum potential will give rise to splitting of the vibrational levels. The degree of splitting will depend upon the height of the potential barrier so that a high barrier will result in only a small splitting. For the rotation of the cyanate ion in an alkali halide lattice,

the barrier to rotation will be greater for the smaller lattice. Thus it is predicted that the splitting will be larger for KI and smaller for KBr, KCl, and NaCl in that order. Upon referring to Table 11 it is seen that this prediction is not verified. Still another objection to this idea is the fact that it predicts that the satellite peaks should be symmetrically placed about the central peak. Since this theory predicts that the ratios of the peaks should be invariant with temperature, cooling the crystals even more would provide a further test.

A third interpretation of these subsidiary peaks is that they may be due to resonance with neighboring cyanate ions. The orientation of the neighboring ion or ions would then determine the direction of the displacement of the fundamental. With this explanation one expects that the effect observed on $NC^{13}O$ in its natural abundance must be due to normal NCO ions since the probability of two $NC^{13}O$ ions being close together is very slight. On the other hand the enriched sample containing 62% C^{13} would contain a relatively large percentage of neighboring carbon-13 ions. Since there is a difference of over 55 cm^{-1} between the C^{13} and C^{12} fundamental, any resonance of perturbation between the two unlike ions should be considerably less than between like ions, so that one would expect the subsidiary peaks, if due to

interaction between C^{12} and C^{13}, to have radically different separations from those due to interaction between two $NC^{12}O$ ions or two $NC^{13}O$ ions. Comparison of Figures 3 and 5 shows that other than resolution there is little difference between the enriched sample and the other sample. There does seem to be a change in resolution which accompanies change in concentration. This latter effect is probably the only result of perturbations by neighboring ions.

What appears to be the best explanation of these peaks is that they may be "hot bands" due to cyanate ions which have one quantum of vibrational motion. Since these peaks are relatively strong at -150°K, and yet higher hot bands are not observed, except possibly in the case of KI, the vibrational frequency seems to be from 150 to 300 cm^{-1}. According to Table 3 the strong band at 93 cm^{-1} for KBr could not be responsible because the Boltzmann factor indicates that the "hot band" for a vibration of this frequency should be about half as strong as the fundamental. In addition since both sum and difference bands are exactly 93 cm^{-1} from the fundamental, the hot band would have to coincide with the fundamental. In KBr two peaks (24 and 25) are found at about 160 cm^{-1} above the fundamental and may give rise to hot bands of the proper intensity. If this hot band theory is correct,

it would not be necessary for the vibrations in question to be infrared active so that even if no suitable absorptions are found, this does not disprove the theory. Since one satellite is above and one below the fundamental, if they are hot bands then either each must be due to a different vibration, one having a negative anharmonicity constant and the other a positive anharmonicity constant, or else the splitting due to the multiple potential minimum discussed above is increased in the excited state. A similar large increase in splitting has been found for excited states of the ammonia molecule.

The remaining fine structure absorptions are most likely due to librations and lattice vibrations. The simplest picture of the possible lattice modes for the cyanate ion in an alkali halide lattice depends largely on the orientation of the cyanate ion. If the cyanate ion is assumed oriented so that the axis of the linear ion is directed along a body diagonal of the unit cell cube then the lattice vibrations can be resolved into those parallel and perpendicular to this axis. The latter should be doubly degenerate vibrations. If we consider the cyanate ion to be nearly a free ion so that the translational and rotational motions are converted to vibrational and librational motions by weak forces, then it is clear that the ion will have only one doubly degenerate

librational mode and two lattice vibrations, one along the axis and the other a doubly degenerate mode perpendicular to the axis of the cyanate ion. The librational bands are expected to be of rather low intensity and might be more diffuse as the librational force constant would probably be quite sensitive to variations in the exact location and orientation of the cyanate ion within the lattice. In addition the intensity of the librational bands would be expected to increase with librational quantum number while the sharpness will probably decrease. Thus the bands T, S, R, and Q are tentatively assigned as librational bands in which T represents the transition from the ground state, S, from the state with one librational quantum, etc. This order is in agreement with the expected decrease in spacing of the librational energy levels with increasing librational quantum number. It also explains why Q is the weakest and broadest peak. On the basis of this interpretation the strength of R and S is rather surprising, but might be ascribed to an increase in intensity of each transition which makes up for the decrease in the number of transitions due to the Boltzmann factor. In the KBr lattice peaks 24 and 25 would be equivalent to S and T, the increase in frequency being expected due to the decrease in lattice dimensions.

For KBr at room temperature peak No. 24 is somewhat broad and there is a similar broad peak at about 2010 cm^{-1} which may be the difference band for which 24 is a sum band. It is also possible that peak 25 in KBr and peak T in KI could be combinations between the fundamental and two quanta of the strong sharp peaks which will next be discussed.

In both KI and KBr a sum and difference band is found which is strong and sharp. In the case of KI this strong band is split. In addition there is a temperature dependent differential in intensity between the nearly degenerate peaks in KI. But for this temperature dependence a multiple potential minimum could be invoked to explain the splitting. Since KBr has a smaller lattice the potential barrier might be high enough to reduce the splitting to a value beyond the resolving power of the spectrometer. These bands (A, B and P, O in KI; and 2 and 21 in KBr) are probably due to lattice vibrations. The decreased lattice dimensions and decreased atomic weights in going from KI to KBr would be expected to shift lattice vibrations to higher frequencies as observed. One possible explanation of the intensity change of the bands P, O and A, B in KI may be a change in selection rules. Perhaps the diminished lattice dimensions or

decreased libration at lower temperatures cause the selection rules to be more rigorous so that the lower frequency peak becomes less active. On this basis the smaller lattice in KBr might make the selection rule even more rigorous so that the lower frequency peak is completely forbidden. The fact that the room temperature strength of this lower peak is stronger than the upper peak might indicate that this is the doubly degenerate lattice mode which is perpendicular to the axis of the ion. It seems reasonable that this lattice mode would be less likely to combine with the stretching fundamental than the mode which is parallel to the axis.

In summary it can be said that, although several explanations are forthcoming in efforts to explain the numerous peaks in the region around the C-N stretching vibrations, so far no set of assignments can be made with confidence.

F. Frequency Shift with Change of Temperature and Lattice

As mentioned above the vibrational frequencies of cyanate ion are found to increase in going from KI to KBr to KCl to NaCl. This change follows the order of decrease in lattice dimensions as shown in Table 13. The change is

Table 13

Variation of Frequency for Cyanate Ion in Various Lattices

Interionic distance (A)		KI 3.53	KBr 3.29	KCl 3.14	NaCl 2.81
$N^{14}C^{12}O^{16}$					
	ν_3	2155.80	2169.60	2181.90	2211.20
	ν_2'	628.0	629.4	631.0	633.2
	ν_1	1200.8	1205.5	1210.7	
	$2\nu_2^\circ$	1288.0	1292.6	1297.3	
$N^{14}C^{13}O^{16}$					
	ν_3	2099.05	2112.80	2124.65	2153.10
	ν_2'	609.95	612.0	613.2	
	ν_1		1191.0		
	$2\nu_2^\circ$	1266.6	1272.5	1277.4	

not the same for all frequencies, nor is it proportional to the frequency. A definite order of magnitude is recognizable for each mode however. The bending mode changes the least, the symmetric stretching mode changes more, and finally the asymmetric stretching mode has the greatest shift with change of alkali halide.

A temperature shift is also discernable and is in the expected direction of increasing frequency with decreasing temperature. This shift is not the same for all frequencies, but does seem to be approximately proportional to the frequency. Tables 14 and 15 show the frequency shifts with temperature for a number of peaks. Figures 13 and 14 plot temperature vs. frequency shift for two halkali halide solutions. Because many of the peaks recorded in Tables 14 and 15 may have their apparent maxima slightly shifted due to overlap with stronger peaks, only the more isolated peaks are plotted on the graphs. It will be noted that for a given alkali halide lattice the temperature dependence is the same for isotopically different ions and for different vibrational states (hot bands and fundamentals). The scattering of the points on the graph is due to the fact that most points are the result of a single measurement and are subject to a relative error of ± 0.2 or 0.3 cm^{-1}.

Table 14

Temperature Dependence of KCl-KNCO Absorption Frequencies

assignment	20°C	0°C	-16°C	-40°C	-65°C	-83°C	-100°C	-135°C	-140°C
$NC^{13}O$	2124.7	2124.9	2124.9	2125.4	2125.7	2125.85	2126.1	2126.6	
$N^{15}CO$	2164.9	2165.0	2165.0	2165.3	2165.6	2165.8	2166.1	2166.4	2166.55
Hot Band for $N^{14}C^{12}O^{16}$	2170.65	2170.7	2171.0	2171.3	2171.7	2171.95	2172.2	----	
NCO^{18}	----	----	----	2173.7	2175.0	2175.1	2175.2	2175.5	2175.7
$N^{14}C^{12}O^{16}$	2181.8	2182.0	2182.0	2182.4	2182.9	2183.1	2183.1	2183.75	

All frequencies given in wave numbers

Figure 13

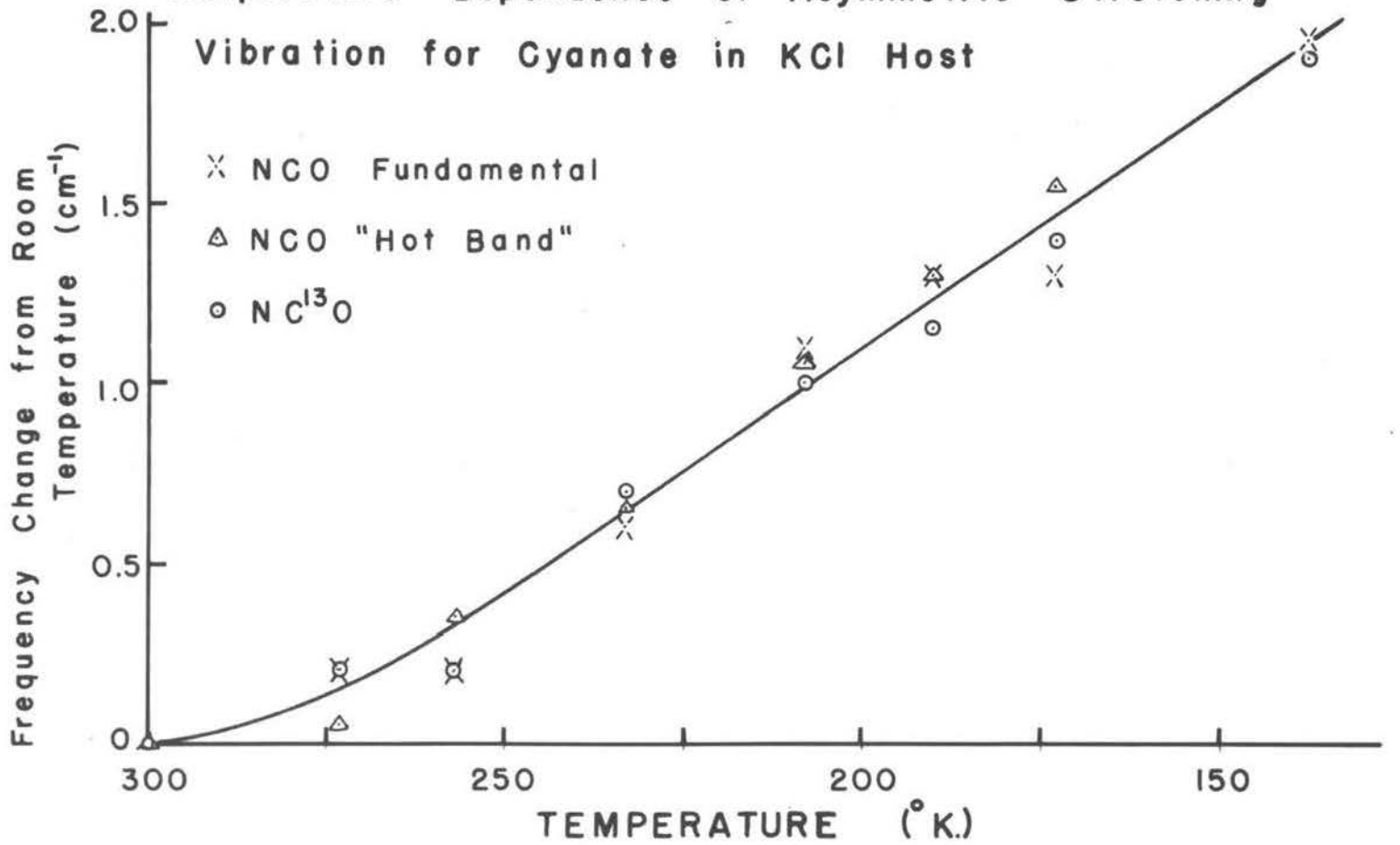
Temperature Dependence of Asymmetric Stretching Vibration for Cyanate in KCl Host
NCO Fundamental
NCO "Hot Band"
NC13O
Frequency Change from Room Temperature (cm-1)
2.0
1.5
1.0
0.5
0
300
250
200
150
TEMPERATURE (°K.)

Table 15

Temperature Dependence of
KBr-KNCO Absorption

Assignment	Temperature (°C.)	Frequency (cm^{-1})
$_{N}{}^{14}C^{12}O^{16}$	+25	2169.60
	-54	2170.24
	-72	2170.14
	-85	2170.70
	-91	2170.65
	-108	2170.73
	-140	2171.14
$_{N}{}^{14}C^{13}O^{16}$	+25	2112.80
	-60	2113.25
	-76	2113.35
	-95	2113.94
	-100	2113.87
	-140	2114.07
Hot band for		
$_{N}{}^{14}C^{12}O^{16}$	+25	2158.55
	-3	2158.55
	-18	2158.73
	-37	2158.77
	-53	2159.25
	-71	2158.95
	-84	2159.30
$_{N}{}^{15}C^{13}O^{16}$	-11	2094.18
	-26	2094.56
	-41	2095.00
	-58	2095.18
	-77	2095.47
	-90	2095.57
	-95	2095.66
	-118	2095.72
	-125	2095.79

Table 15 - Cont.

Assignment	Temperature (°C.)	Frequency (cm^{-1})
Hot band for $N^{14}C^{13}O^{16}$	+25	2102.20
	+2	2102.15
	-11	2102.43
	-28	2102.51
	-42	2102.78
	-58	2102.91
	-76	2102.85
	-92	2103.20
	-95	2103.00

Figure 14

Temperature Dependence of Asymmetric Stretching Vibration for Cyanate in KBr Host

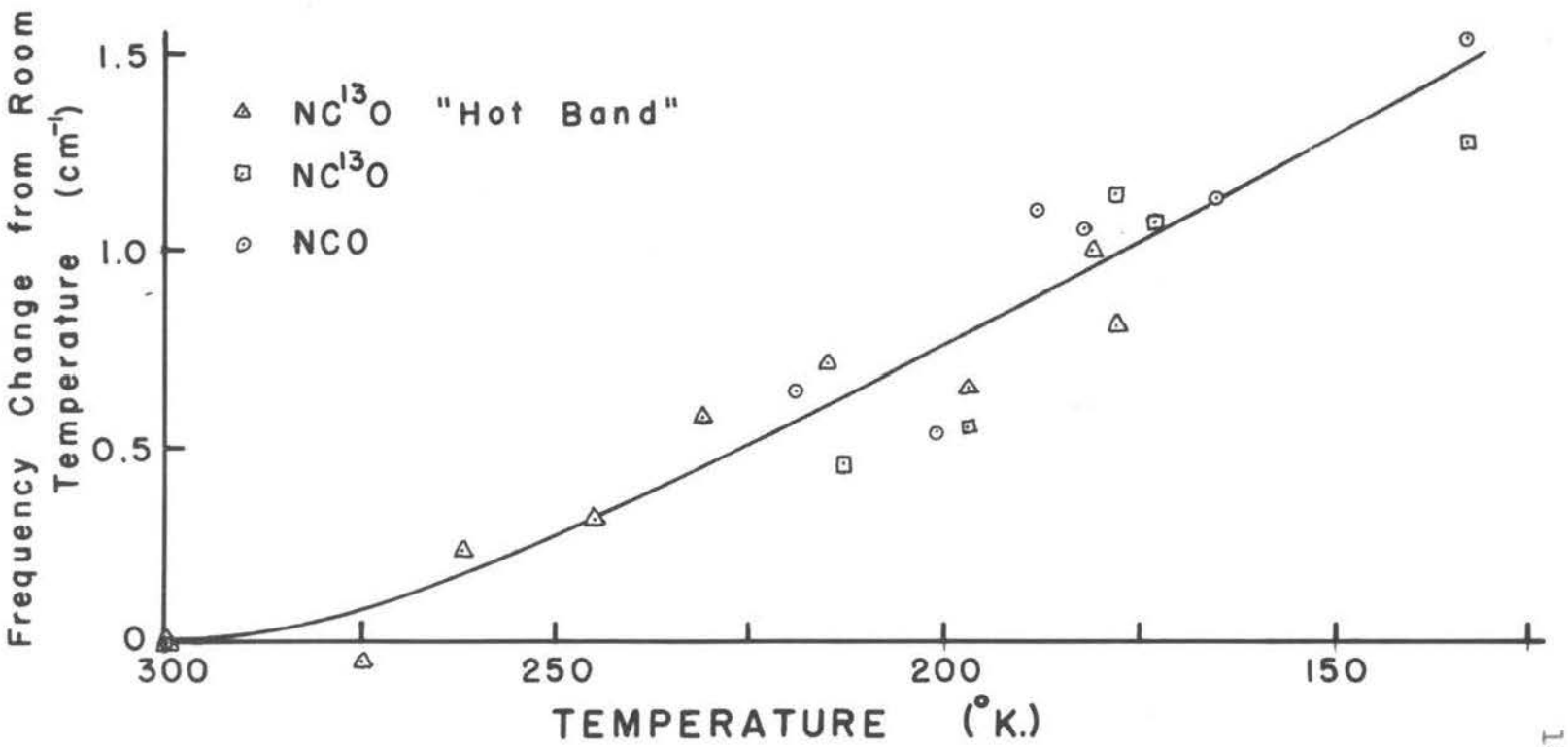

Comparison of the two graphs shows that there is a real difference in the temperature dependence of the two salts measured. One might expect the frequency shift to be related to the coefficient of expansion for the salt, but according to data given in Tables Annuelles (12, p. 20) the salt with the greater coefficient of expansion, KBr, has the smaller change in frequency.

Very likely the frequency shifts are due to two effects resulting from changing lattices. One which is a consequence of decreasing only the lattice dimensions is due to changes in the potential field. Of all the possible long range forces such as dispersion or London forces, Van der Waals forces, and electrostatic forces, none are expected to result in an increase of vibrational frequency. Consequently the shorter range, repulsion forces are probably very important in determining the exact frequency with which the ion vibrates. The other result of change in lattice may be of electrostatic nature. The change from I^- to Br^- to Cl^- will undoubtedly have an effect upon the distribution of electrons within the cyanate ion. Any change in electronic structure of the cyanate ion will in turn affect the force constants of the bonds and consequently change the vibrational frequencies of the ion. This latter effect is more likely

to cause a larger frequency shift for the stronger absorption bands whereas an effect which is due only to changes in lattice dimensions would be more likely to yield a change which is proportional to the frequency. Moreover, the above mentioned changes in electronic distribution due to changes in lattice should strongly affect the zero order frequencies, whereas the changes due to different repulsion forces should have a greater effect on the anharmonicity constants than on the zero order frequencies.

V. POTENTIAL ENERGY OF CYANATE ION

Listed in Tables 16 and 17 are the frequencies of absorptions bands observed for various solid solutions containing cyanate ions in an alkali halide crystal. From these frequencies the anharmonicity constants given in Table 18 have been calculated. Inspection of Table 18 reveals that the two crystals for which the greatest amount of work has been done (KI and KBr) yield calculated anharmonicity constants which are in excellent agreement. In most cases the anharmonicity constants calculated for these two crystals are in agreement within a few tenths of a wave number. Since the anharmonicity constants are calculated, in most cases, as differences between two sums of frequencies, for which each frequency may be in error by several tenths of a wave number, the differences in anharmonicity constant for the two best cases, KI and KBr, are well within experimental error and consequently it is not possible to determine whether there is a genuine change in anharmonicity constant in going from one crystal lattice to another. It does, however, show that any change in these constants due to different crystal lattices must be small. The changes in zero order frequencies are likewise small, but are observable due to the larger size of these potential terms. The Fermi

Table 16

Cyanate Ion in Single Crystals at Room Temperature
April 24, 1958

Assignment lower			Assignment upper			KI	KBr	KCl	NaCl
ν_1	ν_2^ℓ	ν_3	ν_1	ν_2^ℓ	ν_3				
0	0^0	0	0	1'	0	628.0±0.3	629.4±0.3	631.0±0.3	633.2±0.3
0	0^0	0	1	0^0	0	1200.8±0.2	1205.5±0.2	1210.7±0.3	
0	0^0	0	0	2^0	0	1288.0±0.3	1292.6±0.3	1297.3±0.3	
0	0^0	0	0	0^0	1	2155.80±0.10	2169.60±0.10	2181.80±0.10	2211.20±0.2
0	0^0	0	0	4^0	0	2383.6±0.3	2392.9±0.3	2402.8±0.3	
0	0^0	0	1	2^0	0	2477.1±0.2	2487.25±0.2	2498.8±0.3	2520.2±0.5
0	0^0	0	2	0^0	0	2593.8±0.2	2602.5±0.2	2612.8±0.3	
0	0^0	0	0	1'	1	2772.9±0.3	2788.1±0.3	2801.85±0.4	
0	0^0	0	1	0^0	1	3335.6±0.3	3355.0±0.3	3372.6±0.5	
0	0^0	0	0	2^0	1	3422.8±0.3	3442.2±0.3	3458.8±0.5	
0	0^0	0	2	0^0	1	4500±20.	4524.7±10.		
0	0^0	0	1	2^0	1	4590±20.	4623.0±10.		
0	0^0	0	0	4^0	1	4700±20.	4737.5±10.		
0	1'	0	1	0^0	0	569.8±2.0	574.4±2.0		
0	1'	0	0	2^0	0	660.0±0.2	663.2±0.2		

Table 16 - Cont.

Assignment lower ν_1	ν_2'	ν_3	upper ν_1	ν_2'	ν_3	KI	KBr	KCl	NaCl
0	1'	0	1	1'	0	1183.0±0.2	1188.1±0.2	1193.0±0.3	
0	1	0	0	3	0	1304.2±0.3	1309.1±0.3	1314.4±0.3	
0	1'	0	0	1'	1	2144.70±0.10	2158.55±0.10	2170.65±0.10	2200.50±0.3
0	1'	0	0	5'	0				
0	1'	0	1	3'	0				
0	1	0	2	1'	0		2628.25±0.2		
0	1'	0	0	2^2	1	2762.0±0.3	2776.55±0.3		
0	1'	0	1	1'	1	3306.8±0.5	3325.7±0.5	3342.1±0.5	
0	1	0	0	3	1				
0	1'	0	1	0^o	1		2725 ±4.		
0	1	0	0	2^o	1		2813 ±4.		
0	2^2	0	1	2^2	0		1175.5±0.4		
0	2^2	0	0	4^2	0		1320.4±0.4		
0	2^2	0	0	2^2	1	2134.2±0.2	2147.9±0.2	2160.4±0.2	

Table 17

C^{13} Cyanate Ion in Single Crystals at Room Temperature
April 24, 1958

Assignment lower			Assignment upper			KI	KBr	KCl	NaCl
ν_1	ν_2^{ℓ}	ν_3	ν_1	ν_2^{ℓ}	ν_3				
0	0°	0	0	1'	0	609.95±0.5	612.0±0.5	613.2±0.5	
0	0°	0	1	0°	0		1191.0±0.2		
0	0°	0	0	2°	0	1266.6±0.6	1272.5±0.2	1277.4±0.6	
0	0°	0	0	0°	1	2099.05±0.1	2112.80±0.1	2124.65±0.1	2153.10±0.2
0	0°	0	0	4°	0		2360.3±1.0		
0	0°	0	1	2°	0		2462.6±0.2		
0	0°	0	2	0°	0		2554.2±0.2		
0	0°	0	0	1'	1		2714.0±0.3		
0	0°	0	1	0°	1		3284.1±0.5		
0	0°	0	0	2°	1		3366.0±0.5		
0	1'	0	1	0°	0		578.7±2.0		
0	1'	0	0	2°	0		659.1±0.5		
0	1'	0	1	1'	0		1174.4±0.4		
0	1'	0	0	3'	0		1285.7±0.4		

Table 17 - Cont.

Assignment lower			Assignment upper			KI	KBr	KCl
ν_1	ν_2'	ν_3	ν_1	ν_2'	ν_3			
0	1'	0	0	1'	1	2088.4±0.15	2102.20±0.10	2114.05±0.25
0	1'	0	1	1'	1		3257.2±0.5	
0	1'	0	0	3'	1			

Table 18

Anharmonicity Constants Obtained from Observed Frequencies

Constant	KI	KBr	KCl	$NC^{13}O$ in KBr
χ_{11}	-4.35	-4.92	-4.2	-3.3
χ_{22}	-2.70	-2.58	(-11.2)*	(+1.59)*
χ_{33}	---	---	---	---
χ_{12}	+9.20	+9.40	(+44.1)*	(-9.77)*
χ_{13}	-19.8	-18.0	-17.9	-17.8
χ_{23}	-11.10	-11.05	-11.15	-10.6
g_{22}	+2.80	+2.33	(+9.7)*	(-0.31)*
B	61.65_4	61.59	60.82	57.36
b	65.21	65.41	---	---
a	-3.56	-3.82	---	---
ω_1°	1248.15	1254.0	1253.2	1239.0
ω_2°	627.9	629.6_5	(632.5)*	(610.72)*
$\omega_3^\circ + \chi_{33}$	2155.8	2169.6	2181.8	2112.8
ω_1	1253.2	1258.5_5		(1260.97)*
ω_2	634.2_5	635.6_4		(617.72)*
$\omega_3 + 2\chi_{33}$	2176.8	2189.6_5		

* These constants were calculated by a method highly sensitive to slight variations in frequency and are most certainly incorrect due to experimental error

resonance terms also appear to change only slightly, if at all, in going from KI to KBr crystals. It is unfortunate that a similar complete and accurate treatment of KCl and NaCl lattices was not completed, but indications are that here too the anharmonicity and Fermi resonance constants are only slightly changed.

In the case of the isotopic ion $NC^{13}O$ comparison of the observed anharmonicity constants given in Table 18 with those given in Table 19 reveals a few discrepancies which seem too large to be due to experimental error. Upon calculating the vibrational frequencies, however, reasonably close agreement is found between observed and calculated frequencies as shown in Table 8. Nevertheless the differences seem almost too large to be solely due to experimental error and may be due to the little known effects that the solid state has upon the cyanate ion. Since the form of the normal vibrations will be changed in going from one isotopic form to another, the effect of the solid state on the potential function will change in an unknown and unpredictable manner. In addition to this it may be pointed out that even in the case of gaseous carbon dioxide, on which much more work has been done, the agreement between experiment and theory is no better. In fact it is even worse in many instances.

Table 19

Anharmonicity Constants Calculated for a KBr Crystal

Constant	NCO	$NC^{13}O$	$N^{15}CO$	NCO^{18}
ν_1	1249.1	1247.4	1231.2	1210.3
ν_2'	629.4[a]	612.0[a]	626.0_8	624.8
ν_3	2169.6[a]	2112.8[a]	2152.5[a]	2161.5[a]
χ_{11}	-4.92	-4.91	-4.78	-4.62
χ_{22}	-2.58	-2.44	-2.55	-2.54
χ_{33}	-13.0[b]	-12.3	-12.8	-12.89
χ_{12}	+9.4	+9.12	+9.21	+9.04
χ_{13}	-18.0	-17.5	-17.6	-17.3_7
χ_{23}	-11.1	-10.5	-10.9_5	-10.9_7
g_{22}	+2.33	+2.20	+2.31	+2.30
B	61.59	52.78	65.57	66.50
b	65.41	59.72	---	---
a	-3.82	-6.94	---	---
ω_1	1258.5_6	1256.8_8	1240.3_5	1219.2_2
ω_2	635.6_5	617.8	632.3	631.1
ω_3	2215.70	2156.6_5	2197.8_5	2206.9_4

(a) Observed frequencies which were used in the calculations made for this table.
(b) The value of this constant was arbitrarily chosen so as to conform to the expected value.

The force constants calculated for the cyanate ion are given in Table 20. These force constants and the anharmonicity constants given in Table 19 may be used to calculate the vibrational frequencies expected for isotopically different ions. A summary of the results of this type of calculation is included in Table 8. These results substantiate the assignments of a number of observed weak absorption lines as due to various isotopic species.

Table 21 compares the potential constants found for the isoelectronic molecules NCO^-, CO_2, and N_2O. These compounds all have vibrational frequencies and anharmonicity constants of similar magnitude. From this observation one would expect the Fermi resonance constants to be of similar magnitude as they are simply related to the potential constants. This is indeed the case as is also shown in Table 21.

Upon inspection of the spectrum of $NC^{13}O$ one of the most striking features observed is the great difference in intensity found for Fermi resonant doublets. The intensity of the lower frequency peak is always considerably less than that of the higher frequency peak. The separation of the resonance doublets is, however, found to be approximately the same as for the normal $NC^{12}O$

Table 20

Force Constants for the Cyanate Ion

KBr crystals containing cyanate ions

K_{CN} = 15.879 mdynes/Å		
K_{CO} = 11.003 mdynes/Å		
K_{12} = 1.422 mdynes/Å		from $NC^{13}O$
$K^*_{\alpha/l_1 l_2}$ = 0.5086 mdynes/Å		0.5083 mdynes/Å
K^*_{α} = 0.7319 mdynes Å/radian		0.7315 mdynes Å/radian

KI crystals containing cyanate ions

K_{CN} = 15.512 mdynes/Å

K_{CO} = 11.028 mdynes/Å

K_{12} = 1.352 mdynes/Å

$K^*_{\alpha/l_1 l_2}$ = 0.5063 mdynes/Å

K^*_{α} = 0.7286 mdyne Å/radian

Less reliable force constants calculated using linear equations only for cyanate in KBr

K_{CN} = 15.424 mdynes/Å

K_{CO} = 11.523 mdynes/Å

K_{12} = 1.454 mdynes/Å

* assuming l_{CN} = 1.17 Å and l_{CO} = 1.23 Å obtained upon application of Badger's Rule

Table 21

Comparison of Anharmonicity Constants for Cyanate, Carbon Dioxide, and Nitrous Oxide

Constant	Average value for NCO^- in KBr, KI, and KCl	CO_2 [a]	N_2O [b]
χ_{11}	-4.49	-2.61	-5.21
χ_{22}	-2.64	-0.75	-0.17
χ_{33}	---	-12.50$_4$	-15.04
χ_{12}	+9.3	+3.76	+0.52
χ_{13}	-18.6	-19.17	-27.29
χ_{23}	-11.1	-12.42	-14.23
g_{22}	+2.56	+1.03	+0.52
B	61.62	72.14	40
ω_1°	1254.04 [c]	1345	1282.11
ω_2°	629.65 [c]	667.02	588.43
ω_3°	2182.60 [c]	2361.80	2238.79

[a] According to Taylor, Benedict, and Strong (48, p. 1896-1898) as revised by Herzberg and Herzberg (28, p. 1039-1040)

[b] According to Grenier-Besson and Amat (22, p. 2067-2068) as revised by Plyler, Tidwell, and Allen (42, p. 97)

[c] Values found for KBr lattice using constants given in Table 19

ion. This inequality of intensities must be due to one of two possible causes, a) the intensities of the unperturbed absorptions must change quite radically in going from one isotopic species to another or b) the unperturbed bands must be farther apart while the Fermi resonance constant must be smaller in order to give a spacing comparable to that for the $NC^{12}O$ ion. Calculations indicate that the latter alternative is the principle cause. Upon referring back to the equation for the Fermi resonance constant (see page 36) it is seen that in going from $NC^{12}O$ to $NC^{13}O$ the resonance constant is expected to increase. This is contrary to the observed fact. The explanation must lie in the fact that the constant b is in actuality a linear combination of two potential constants. As the mass weighted geometry of the molecule is altered in going from one ionic species to another, the form of the linear combination will change and consequently the value of b will change. If b were measured accurately for both $NC^{12}O$ and $NC^{13}O$ it would be possible to calculate the two potential constants from these values. Since there are other factors involved due to the fact that we are here dealing with solids rather than isolated ions, this type of calculation would be meaningless. It does, however, show that b need not be expected to increase

in value upon going from $NC^{12}O$ to $NC^{13}O$. Stoicheff (47, p. 218-230) has found a similar decrease in Fermi res. constant in going from $C^{12}O_2$ to $C^{13}O_2$.

Returning to the values of the force constants and referring to Table 22 it is seen that the magnitude of these force constants indicates that the C-N bond is

Table 22

Typical Values of Force Constants for Different Bond Orders (53, p. 175)

bond	force constant (md/Å)
C - O	5.0 -- 5.8
C = O	11.8 -- 13.4
C - N	4.0 -- 5.6
C = N	10 -- 11
C ≡ N	16.2 -- 18.2

largely a triple bond while the C-O bond has a great deal of single bond character. The use of Badger's rule (7, p. 710-714) to determine the bond distances given in Table 20 makes it possible to compare the bond distances indicated by this work with those obtained by Bassière from X-ray data. This comparison seems to indicate that Bassière is in error in reporting the C-N bond distances to be the larger, and the C-O bond distances to be the

smaller of the two. In-as-much as it is difficult to distinguish between oxygen and nitrogen atoms in x-ray diffraction work, an error of this type is not too improbable. While it is true that Badger's rule is only an empirical approximation, nevertheless the rule has been found to be good to within ± 0.02 Å for many compounds.

By the use of Pauling's formula for determining the relative importance of resonance structures (40, p. 195) the percentage contribution of each resonant structure has been calculated to be as follows:

I	$N \equiv C - O^-$	76%
II	$N^- = C = O$	6%
III	$N^{-2} - C \equiv O^{+1}$	18%

This is closely parallel to the results found by L. Jones (32, p. 1072) in the case of the similar thiocyanate ion for which the respective percentages are 71%, 12%, and 17%. As a matter of fact the increased contribution of structure I over structures II and III is just what would be predicted for cyanate ion because oxygen is more electronegative than sulfur.

APPENDIX I

Calculation of Potential Constants

Using the observed frequencies given in tables 16 and 17 the anharmonicity constants x_{ij} given in table 18 have been calculated using the equation

$$\nu_0 = E - E_0 = \sum_{i=1}^{3} \omega_i^\circ \nu_i + \sum_{k \le i = 1}^{3} x_{ik} \nu_i \nu_k + g_{22} \ell_2^2$$

From these ω_i° the zero-order frequencies ω_i have been determined by the equation

$$\omega_i = \omega_i^\circ - x_{ii} d_i - \tfrac{1}{2} \sum_{k \neq i} x_{ik} d_k$$

where d_k is the degeneracy of the kth normal coordinate.

Table 19 lists the anharmonicity constants for various isotopic species of the cyanate ion in KBr. The constants in the first column of this table are those obtained directly from observed frequencies given in Table 16. The remaining columns contain the values calculated from the empirical relation (27, p. 229)

$$x'_{ij} = \frac{\omega'_i \, \omega'_j}{\omega_i \, \omega_j} \, x_{ij}$$

where the prime denotes a different isotopic species.

Because it was not possible to detect any overtones

or combinations involving $v_3 > 1$, it was not possible to determine the value of x_{33}. Instead, a value of $x_{33} = -13.0$ was assumed for $N^{14}C^{12}O^{16}$ by comparison with the values found for CO_2 and N_2O (see Table 21).

In order to obtain the ω_i's for the isotopic species other than $N^{14}C^{12}O^{16}$ it was first necessary to approximate the x_{ij}'s and calculate the approximate zero-order frequencies from the observed frequencies. These approximate zero-order frequencies were then used to arrive at more exact x_{ij}'s from which more exact zero-order frequencies could be calculated. Anharmonicity constants calculated from these more refined zero-order frequencies were not significantly different so that further refinement was deemed unnecessary.

Since the value of v_1 could not be reliably determined from observed frequencies for any isotopic species other than $N^{14}C^{12}O^{16}$, the Redlich-Teller product rule was utilized to obtain the value of ω_1 from which v_1 was calculated using the anharmonicity constants. These values are also recorded in Table 19.

The stretching force constants were calculated from the zero-order frequencies using the equations

$$\lambda_1 + \lambda_3 = k_{cN}\mu_N + k_{co}\mu_o + (k_{cN} + k_{co} - 2k_{12})\mu_c \qquad (1)$$

$$\lambda_1 \lambda_3 = (k_{CN} k_{CO} - k_{12}^2)(\mu_N \mu_C + \mu_C \mu_O + \mu_N \mu_O) \qquad (2)$$

where $\mu_i = \frac{1}{m_i}$ and $\lambda_i = 4\pi^2 \nu_i^2 c^2$

Using the linear equations only, it is possible to obtain unambiguous values for the force constants. The use of the linear equations, however, requires an exact knowledge of λ_1 and λ_3 for at least three isotopic species. In-as-much as the ν_i must be calculated with the aid of the Redlich-Teller product for all except $N^{14}C^{12}O^{16}$, and because the zero-order frequencies for $N^{14}C^{12}O^{16}$ and $N^{14}C^{13}O^{16}$ are deemed more reliable, the force constants obtained from these frequencies using both equations given above are considered more reliable. Because the use of quadratic equations introduces spurious roots, the roots of the linear equations were used to determine which roots were superfluous.

Using the empirical Badger's rule (7, p. 710-714)

$$R = \frac{1.230}{(k)^{1/3}} + 0.68$$

where R is the bond distance in Angstroms and k is the stretching force constant in millidynes/Å, the bond distances for the cyanate ion were calculated and are recorded in Table 20. The bending force constant was then calculated using these bond distances in the equation

$$\lambda_2 = k_\alpha \left[\frac{\mu_N}{R_{CN}^2} + \frac{\mu_O}{R_{CO}^2} + \mu_C \left(\frac{1}{R_{CN}} + \frac{1}{R_{CO}} \right)^2 \right]. \qquad (3)$$

In the case of the salts NaNCO and KNCO the bending force constant was calculated using equation (3), the observed frequencies rather than zero-order frequencies, and the bond distances previously found using Badger's rule rather than the x-ray distances found by Pauling and Bassière.

APPENDIX II

Fermi Resonance Calculation

In the section on Fermi resonance it was shown that the perturbed frequencies w are given by the equation

$$\begin{vmatrix} W_1^\circ - W & W_{12} \\ W_{12} & W_2^\circ - W \end{vmatrix} = 0$$

for the Fermi resonant doublets and by the equation

$$\begin{vmatrix} W_1^\circ - W & W_{12} & W_{13} \\ W_{12} & W_2^\circ - W & W_{23} \\ W_{13} & W_{23} & W_3^\circ - W \end{vmatrix} = 0$$

for Fermi resonant triplets.

The evaluation of the off-diagonal terms is discussed on pages 36 and 37. In the calculations used to obtain the Fermi resonance constants reported in Tables 18, 19, and 21 our b is the same as that of Dennison (17, p. 179-188) and is related to the normal coordinate potential constant g_{122} by the equation

$$b = \frac{h^{3/2}}{16\pi^3 \omega_1^{1/2} \omega_2} v_1^{1/2} \left[(v_2+2)^2 - \ell^2\right]^{\frac{1}{2}} g_{122} .$$

The a is a constant related to the quintic potential constant g_{12222} by the relation

$$a = \frac{h^{5/2}}{32\pi^5 \omega_1^{1/2} \omega_2^2} v_1^{1/2} (v_2+2)\left[(v_2+2)^2 - \ell^2\right]^{\frac{1}{2}} g_{12222} .$$

Consequently

$$W_{12} = W_{100,02^{2}0} = -\frac{1}{\sqrt{2}}(b + a)$$

$$W_{12} = W_{11'0,03'0} = -(b + 3/2\, a)$$

etc.

In calculations which ignore the quintic term and consequently also "a" the Fermi resonance is described by the term B where

$$W_{12} = W_{100,02^{2}0} = -\frac{B}{\sqrt{2}}$$

$$W_{12} = W_{11'0,03'0} = -B$$

etc.

BIBLIOGRAPHY

1. Acampora, Fred M., Albert S. Tompa and Norman O. Smith. Homogenization of solid solutions. A proposed new technique. The Journal of Chemical Physics 24:1104. 1956.

2. Adel, Arthur and David M. Dennison. The infrared spectrum of carbon dioxide. Part I. Physical Reviews 43:716-723. 1933.

3. Adel, Arthur and David M. Dennison. The infrared spectrum of carbon dioxide. Part II. Physical Reviews 44:99-104. 1933.

4. Allen, Harry C., L. R. Blaine and Earle K. Plyler. Vibrational constants of acetylene-d_2. Journal of Research of the National Bureau of Standards 56: 279-283. 1956.

5. Allen, Harry C., Eugene D. Tidwell and Earle K. Plyler. Inrared spectra of hydrogen cyanide and deuterium cyanide. The Journal of Chemical Physics 25:302-307. 1956.

6. Angus, W. R. et al. Structure of benzene. VIII. Assignment of vibration frequencies of benzene and kexadeuterobenzene. Journal of the Chemical Society 1936:971-987. 1936.

7. Badger, R. M. The relation between the internuclear distances and force constants of molecules and its application to polyatomic molecules. The Journal of Chemical Physics 3:710-714. 1935.

8. Bassière, Marc. Structure crystalline des azotures. La constitution de l'anion. Comptes Rendus de Séances de l'Académie des Sciences 208:659-661. 1939.

9. Bassière, Marc. Sur la structure de l'isocyanate de sodium. Comptes Rendus de Séances de l'Académie des Sciences 206:1309-1311. 1938.

10. Buckley, H. Crystal growth. New York, Wiley, 1951. 571 p.

11. Cleveland, Forrest F. Raman spectrum of an aqueous solution of potassium cyanate. Journal of the American Chemical Society 63:622-623. 1941.

12. Comité International nommé par le VII^{e} Congrés de Chimie Appliquée. Tables annuelles de constantes et données numériques de chimie, de physique, de biologies et de technologie. Publiées sous le patronage de l'Union de Chemie Pure et Appliquée. Vol. 7. Part 1. Paris, Gauthier-Villars, 1930. 946 p.

13. Cook, Ralph P. and Percy L. Robinson. Certain physical properties of cyanogen and its halides. Journal of the Chemical Society 1935:1001-1005. 1935.

14. Decius, John Courtney. Coupling of the out-of-plane bending mode in nitrates and carbonates of the aragonite structure. The Journal of Chemical Physics 23:1290-1294. 1955.

15. Decius, John Courtney. Intermolecular coupling of the out-of-plane bending mode of several carbonates. The Journal of Chemical Physics 22:1946. 1954.

16. Decius, John Courtney. N^{15} isotope shift of the perpendicular bending frequency in KNO_3 and $NaNO_3$. The Journal of Chemical Physics 22:1941. 1954.

17. Dennison, David M. The infra-red spectra of polyatomic molecules. Part II. Reviews of Modern Physics 12:175-214. 1940.

18. Downie, A. R. et al. The calibration of infrared prism spectrometers. Journal of the Optical Society of America 43:941-951. 1953.

19. Dows, David A. Calibration of infrared prism spectrometers. Journal of the Optical Society of America 48:73. 1958.

20. Fermi, Enrico. Über den Ramaneffekt des Kohlendioxyds. Zeitschrift für Physik 71:250-259. 1931.

21. Fredericks, William John. An investigation of solid alkali halide phosphorus. Ph. D. thesis. Corvallis, Oregon State College, 1956. 132 numb. leaves.

22. Grenier-Besson, Marie Louise and Gilbert Amat. Sur l'étude théorique du spectre de vibration de l'oxyde azoteux. Comptes Rendus de Séances de l'Académie des Sciences 238:2067-2068. 1954.

23. Gonbeau, J. Raman-effect und das Konstitutions -- problem des Cyanat-restes. (XXX. Mitteil) Zur Kenntnis der Pseudohalogene. Berichte der Deutschen Chemischen Gesellshaft 68:912-919. 1935.

24. Haas, C. and J. A. A. Ketelaar. The effective field and the frequency of overtones and combination bands in the vibration spectra of crystals. Physica 22: 1286-1290. 1956.

25. Halford, Ralph S. Motions of molecules in condensed systems: I. Selection rules, relative intensities, and orientation effects for Raman and infra-red spectra. The Journal of Chemical Physics 14:8-15. 1946.

26. Hendricks, Sterling B. and Linus Pauling. The crystal structures of sodium and potassium trinitrides and potassium cyanate and the nature of the trinitride group. Journal of the American Chemical Society 47:2904-2920. 1925.

27. Herzberg, Gerhard. Molecular spectra and molecular structure. II. Infrared and Raman spectra of polyatomic molecules. New York, Van Nostrand, 1945. 632 p.

28. Herzberg, Gerhard and L. Herzberg. Rotation-vibration spectra of diatomic and simple polyatomic molecules with long absorbing paths. XI. The spectrum of carbon dioxide (CO_2) below 1.25μ. Journal of the Optical Society of America 43:1037-1044. 1953.

29. Hexter, R. M. and David A. Dows. Low-frequency librations and the vibrational spectra of molecular crystals. The Journal of Chemical Physics 25:504-509. 1956.

30. Hofmann, K. A. et al. Oxydation von gebundenem Stickstoff zu Salpeter bei niederen Temperaturen und reduction von Salpeter zum cyanid. Berichte der Deutschen Chemischen Gesellshaft 59:204-212. 1926.

31. Hornig, Donald F. The vibrational spectra of molecules and complex ions in crystals. I. General theory. The Journal of Chemical Physics 16:1063-1076. 1948.

32. Jones, Llewellyn H. Infrared spectrum and structure of the thiocyanate ion. The Journal of Chemical Physics 25:1069-1072. 1956.

33. Jones, Llewellyn H. Polarized infrared spectrum of potassium thiocyanate. The Journal of Chemical Physics 28:1234-1236. 1958.

34. Kimura, Katsumi and Masao Kimura. Approximate method in calculating mean-square amplitudes of bonded interatomic distances. The Journal of Chemical Physics 25:362. 1956.

35. Kyropoulos, S. Dielektrizitätskonstanten regulärer Kristalle. Zeitschrift für Physik 63:849-854. 1930.

36. Kyropoulos, S. Ein Verfahren zur herstellung groszer Kristalle. Zeitschrift für Anorganische und Allgemeine Chemie 154:308-313. 1926.

37. Newman, Roger and Ralph S. Halford. Motions of molecules in condensed systems. VII. The infrared spectra of single crystals of NH_4NO_3 and $TlNO_3$ in polarized radiation. The Journal of Chemical Physics 18:1276-1290. 1950.

38. Newman, Roger and Ralph S. Halford. Motions of molecules in condensed systems. VIII. Infrared spectra for NH_4NO_3, $TlNO_3$, $Pb(NO_3)_2$ at -160° and 25°C. The Journal of Chemical Physics 18:1291-1294. 1950.

39. Pal, N. N. and P. N. Sen Gupta. Raman effect in some organic and inorganic substances. Indian Journal of Physics 5:13-34. 1930.

40. Pauling, Linus. The nature of the chemical bond. 2d ed. Ithaca, Cornell University Press, 1948. 450 p.

41. Plyler, Earle K., L. R. Blaine and W. S. Conner. Velocity of light from the molecular constants of carbon monoxide. Journal of the Optical Society of America 45:102-106. 1955.

42. Plyler, Earle K., Eugene D. Tidwell and Harry C. Allen, Jr. Near infrared spectrum of nitrous oxide. The Journal of Chemical Physics 24:95-97. 1956.

43. Porterin, A. Sur la dècomposition du cyanate de potassium par la chaleur. Comptes Rendus de séances de l'Académie des Sciences 161:308-310. 1915.

44. Redlich, Otto. Eine allgemeine Beziehung zwischen den Schwingungs-frequenzen isotoper Molekeln. Zeitschrift für Physikalische Chemie B28:371-382. 1935.

45. Slykhouse, T. E. and H. O. Drickamer. Effect of pressure on CN^- dissolved in an alkali halide lattice. The Journal of Chemical Physics 27:1226-1227. 1957.

46. Stimson, Miriam Michael and Marie Joannes O'Donnell. The infrared and ultraviolet absorption of cytosine and isocytosine in the solid state. Journal of the American Chemical Society 74:1805-1808. 1952.

47. Stoicheff, B. P. High resolution Raman spectroscopy of gases. XI. Spectra of CS_2 and CO_2. Canadian Journal of Physics 36:218-230. 1958.

48. Taylor, J. H., W. S. Benedict and J. Strong. Infrared spectra of H_2O and CO_2 at 500°C. The Journal of Chemical Physics 20:1884-1898. 1952.

49. Wagner, E. L. and Donald F. Hornig. The vibrational spectra of molecules and complex ions in crystals. III. Ammonium chloride and deutero-ammonium chloride. The Journal of Chemical Physics 18:296-304. 1950.

50. Walnut, Thomas H. A study of selection rules for vibrational spectra of complex crystals. The Journal of Chemical Physics 20:58-62. 1952.

51. Walsh, A. Multiple monochromators. II. Application of a double monochromator to infrared spectroscopy. Journal of the Optical Society of America 42:96-100. 1952.

52. Williams, Dudley. The infrared spectrum of potassium cyanate solutions. Journal of the American Chemical Society 62:2442-2444. 1940.

53. Wilson, E. Bright, Jr., John Courtney Decius and Paul C. Cross. Molecular Vibrations. New York, McGraw-Hill, 1955. 388 p.

54. Winston, H. and Ralph S. Halford. Motions of molecules in condensed systems. V. Classification of motions and selection rules for spectra according to space symmetry. The Journal of Chemical Physics 17:607-616. 1949.

55. Wu, Ta-You. Vibrational spectra and structure of polyatomic molecules. 2d ed. Ann Arbor, J. W. Edwards, 1946. 335 p.